Studies in Radar Cross-Sections VI

UMM-106 = RL-2014

Cross-Sections of Corner Reflectors and Other Multiple Scatterers at Microwave Frequencies

by R.R. Bonkowski, C.R. Lubitz, and C.E. Schensted

Project MIRO
Contract No. AF 30(602)-9

Willow Run Research Center
Engineering Research Institute
University of Michigan
UMM-106 October, 1953

FOR INTRA-UNIVERSITY CORRESPONDENCE

UNIVERSITY OF MICHIGAN

ENGINEERING RESEARCH INSTITUTE

21 February 1958

MEMO TO: Prof. K. M. Siegel

FROM: Security Office

SUBJECT: Project 2015

This is to advise you that all reports and memos generated on Project 2015 (AF30(602)9 are unclassified.

Please see that all documents in your possession are marked in the manner illustrated below. Regrading markings should appear on front and back covers, title, first and last pages, with the previous classification lined through.

CLASSIFICATION
CHANGED TO
UNCLASSIFIED
AS PER AUTHORITY
change order RADC
14 Aug 56 - R.B. McInerney

Bulk files of aforementioned reports need not be so marked immediately. Regrading markings can be affixed when the documents are being used or charged out or transmitted. However, if bulk files are in your possession, the change of classification should be indicated inside the file drawer or storage container.

V. J. SCOTIUS
Security Officer

fg
c.c.: J. H. Richter

Studies in Radar Cross-Sections - VI: Cross-Sections of Corner Reflectors and Other Multiple Scatterers at Microwave Frequencies by R. R. Bonkowski, C. R. Lubitz, and C. E. Schensted (UMM-106, October 1953; Reprinted June 1954). Contract No. AF 30(602)-9. SECRET (UNCLASSIFIED when Appendix is removed).

Errata in First Printing

Pg. 11, Eq. 2.4-3	Replace $\hat{k} + 2(\hat{k}$ .... by $\hat{k} - 2(\hat{k}$ ....
Pg. 16,	Caption on the horizontal scale should be γ DEGREES
Pg. 39, Eq. 3.4-6	The last term should be $(z + b_1)^2 \, d\phi^2$
Pg. 41, line below Eq. 3.4-16	Replace "For $\phi = \theta$ .... by "For $\phi = 0$ ....

Errata in Second Printing

Pg. 39, Eq. 3.4-6	Same as in 1st printing
Pg. 41, line below Eq. 3.4-16	Same as in 1st printing

Addenda

None

TABLE OF CONTENTS

MISSING
PAGE

MISSING
PAGE

NOMENCLATURE

The symbol for a vector is an arrow over the letter, e.g., $\vec{R}$. The unit vector parallel to $\vec{R}$ is written as $\hat{R}$ while R stands for the magnitude of $\vec{R}$. Thus $\vec{R} = R\hat{R}$.

The subscripts i and s stand for incident and scattered respectively.

$e^{-i\omega t}$ time dependence is used throughout.

The transpose of a matrix is represented by a tilde. Thus the transpose of M is $\tilde{M}$.

SYMBOL	MEANING	SECTION FIRST USED IN
$\hat{a}$	$\hat{a} = \frac{\vec{H}_i}{H_i} = a_x \hat{i}_x + a_y \hat{i}_y + a_z \hat{i}_z$	2.4
$\hat{a}_H$	$\hat{a}_H = -\frac{1}{\sqrt{2}} \hat{i}_x + \frac{1}{\sqrt{2}} \hat{i}_y$	2.4
A	Area of equivalent aperture	2.1
b	Side length of a corner reflector	2.3
b_1	Smallest radius of the cones in a biconical reflector	3.4
b_2	Largest radius of the cones in a biconical reflector	3.4
B	Radius of gyration	2.1
c	Velocity of light	2.4
c_1, c_2, c_3	Defined in Eq. (2.4-9)	2.4
d	Distance between two spheres	3.2
D	Cross-sectional area of a bundle of rays	3.1
$\vec{E}$	Electric field	3.1
E,F,G	$\hat{k} + \hat{R} = E \hat{i}_x + F \hat{i}_y + G \hat{i}_z$	2.4
g_{pq}	$d\sigma^2 = g_{uu}\, du^2 + 2g_{uv}\, dudv + g_{vv} dv^2$ and $g_{uv} = g_{vu}$	3.1

g^{pq}	$\begin{bmatrix} g^{uu} & g^{uv} \\ g^{vu} & g^{vv} \end{bmatrix} = \frac{1}{g_{uu}g_{vv} - g_{uv}^2} \begin{bmatrix} g_{vv} & -g_{uv} \\ -g_{vu} & g_{uu} \end{bmatrix}$	3.1
G_{pq}	$G_{pq} = -\frac{\partial n_x}{\partial p}\frac{\partial x}{\partial q} - \frac{\partial n_y}{\partial p}\frac{\partial y}{\partial q} - \frac{\partial n_z}{\partial p}\frac{\partial z}{\partial q}$	3.1
h	The characteristic dimension of a body	2.1
$\vec{H}$	The magnetic field	2.1
$\hat{H}_N$	A unit vector parallel to the N-tuply scattered field	3.3
$\hat{i}_x, \hat{i}_y, \hat{i}_z$	Unit vectors along the x, y, and z axes	2.4
I	$I = \int_{-\infty}^{\infty} \cdots \int_{-\infty}^{\infty} e^{ik\tilde{\xi} M \xi} d\xi_1 \ldots d\xi_{2N}$	3.3
k	$k = 2\pi/\lambda$	2.1
$\hat{k}$	$\hat{k} = \frac{\vec{E}_i \times \vec{H}_i}{\lvert \vec{E}_i \times \vec{H}_i \rvert}$	2.4
K	$\sigma = Kb^n$	IV
ℓ, m, n	Direction cosines between the direction to the transmitter and the axes of a corner reflector	2.3
M	Defined in Eq. (3.3-8)	3.3
n	$\sigma = Kb^n$	IV
$\hat{n}$	Unit outward normal to surface $= n_x\hat{i}_x + n_y\hat{i}_y + n_z\hat{i}_z$	2.1
$\hat{n}_j$	Unit normal on the j'th reflecting surface	3.3
N	Number of reflecting surfaces	3.3
p, q	May equal either u or v	3.1
r_o	Radius of a sphere	3.2
$\vec{r}$	Radius vector from origin to integration point	2.1

$\vec{r}_j$	Radius vector from arbitrary reference point to a point on the j'th reflecting surface	3.3
R_1	Distance from specular reflection point on upper cone or from left hand sphere	3.2
$\vec{R}$	Vector from origin to field point = $R\hat{R}$	2.1
$\hat{R}$	Unit vector from origin to field point = $R_x\hat{i}_x + R_y\hat{i}_y + R_z\hat{i}_z$	2.1
$\vec{R}_j$	Vector from the j'th reflection point to the $(j+1)^{st}$ reflection point	3.3
$\vec{R}_N$	Vector from the N'th reflection point to the field point	3.3
$\vec{R}'$	Vector from integration point to field point	2.1
S	Surface of scattering body	2.1
s_1, s_2, s_3	Defined in Eq. (2.4-9)	2.4
t	Time	2.4
T_{pq}	$T_{pq} = g_{pq} - \Omega_p \Omega_q + R(\Omega_{pq} - \cos \zeta\ G_{pq})$	3.1
T^p_q	$T^p_q = g^{pu} T_{uq} + g^{pv} T_{vq}$	3.1
u, v	Curvilinear coordinates on the scattering surface	3.1
w	May equal either u or v	3.1
x,y,z	Cartesian coordinates	2.4
$\alpha_{j11}, \alpha_{j12}, \alpha_{j21}, \alpha_{j22}$	Cosine of the angle between the x_j and x_{j+1}, x_j and y_{j+1}, y_j and x_{j+1}, and y_j and y_{j+1} axes respectively	3.3
β	$\cos \beta = R_z$	2.4
γ	$\tan \gamma = \frac{R_y}{R_x}$	2.4

Γ^{p}_{qw}	Christoffel symbol of the second kind $\Gamma^{p}_{qw} = g^{pu}\left[q,w;u\right] + g^{pv}\left[q,w;v\right]$	3.1
δ	Angle between symmetry axis of corner reflector and direction to transmitter in degrees	2.3
Δ	Measure of constructional error	2.5
ζ	Angle of incidence	3.1
$\theta_1, \theta_2, \theta_j$	Polar Angles	3.2
λ	Wavelength	2.1
ξ	$\xi = \left[\xi_1, \xi_2, \xi_3, \ldots \xi_{2N}\right]$	3.3
ξ_j	$\xi_{2j} = y_j$ and $\xi_{2j-1} = x_j$	3.3
ρ	Radius of curvature	3.3
σ	Radar cross-section	2.1
$d\sigma$	Element of arc length	3.1
τ	$\tau = \frac{\pi b}{\lambda}\left[\frac{1}{\sqrt{2}}\sin\beta - \cos\beta\right]$	2.4
$\delta\psi$	Angle between center of beam and half-power point	2.1
$\phi, \phi_1, \phi_2, \phi_j$	Azimuth angles	3.2
ω	$\omega = kc = \frac{2\pi c}{\lambda}$	2.4
Ω	$e^{ik\,\Omega(u,v)}$ is the phase factor for a wave incident on a surface	3.1
Ω_p	$\Omega_p = \frac{\partial \Omega}{\partial p}$	3.1

Ω_{pq} $\qquad \Omega_{pq} = \dfrac{\partial^2 \Omega}{\partial p\, \partial q} - \Gamma^{u}_{pq} \dfrac{\partial \Omega}{\partial u} - \Gamma^{v}_{pq} \dfrac{\partial \Omega}{\partial v}$ $\qquad$ 3.1

$[p,q;\, w]$ $\qquad$ Christoffel symbol of the first kind $\qquad$ 3.1

$$[p, q; w] = \frac{1}{2} \left(\frac{\partial g_{pw}}{\partial q} + \frac{\partial g_{qw}}{\partial p} - \frac{\partial g_{pq}}{\partial w} \right)$$

PREFACE

This paper is the sixth in a series of reports growing out of studies of radar cross-sections at the University of Michigan's Willow Run Research Center. The primary aims of this program are:

(1) To show that radar cross-sections can be determined analytically.

(2) To elaborate means for computing cross-sections of objects of military interest.

(3) To demonstrate that these theoretical cross-sections are in agreement with experimentally determined values.

Intermediate objectives are:

(1) To compute the exact theoretical cross-sections of various simple bodies by solution of the appropriate boundary-value problems arising from the electromagnetic vector wave equation.

(2) To examine the various approximations possible in this problem, and determine the limits of their validity and utility.

(3) To find means of combining the simple body solutions in order to determine the cross-sections of composite bodies.

(4) To tabulate various formulas and functions necessary to enable such computations to be done quickly for arbitrary objects.

(5) To collect, summarize, and evaluate existing experimental data.

Titles of the papers already published or presently in process of publication are listed on the back of the title page.

K. M. Siegel

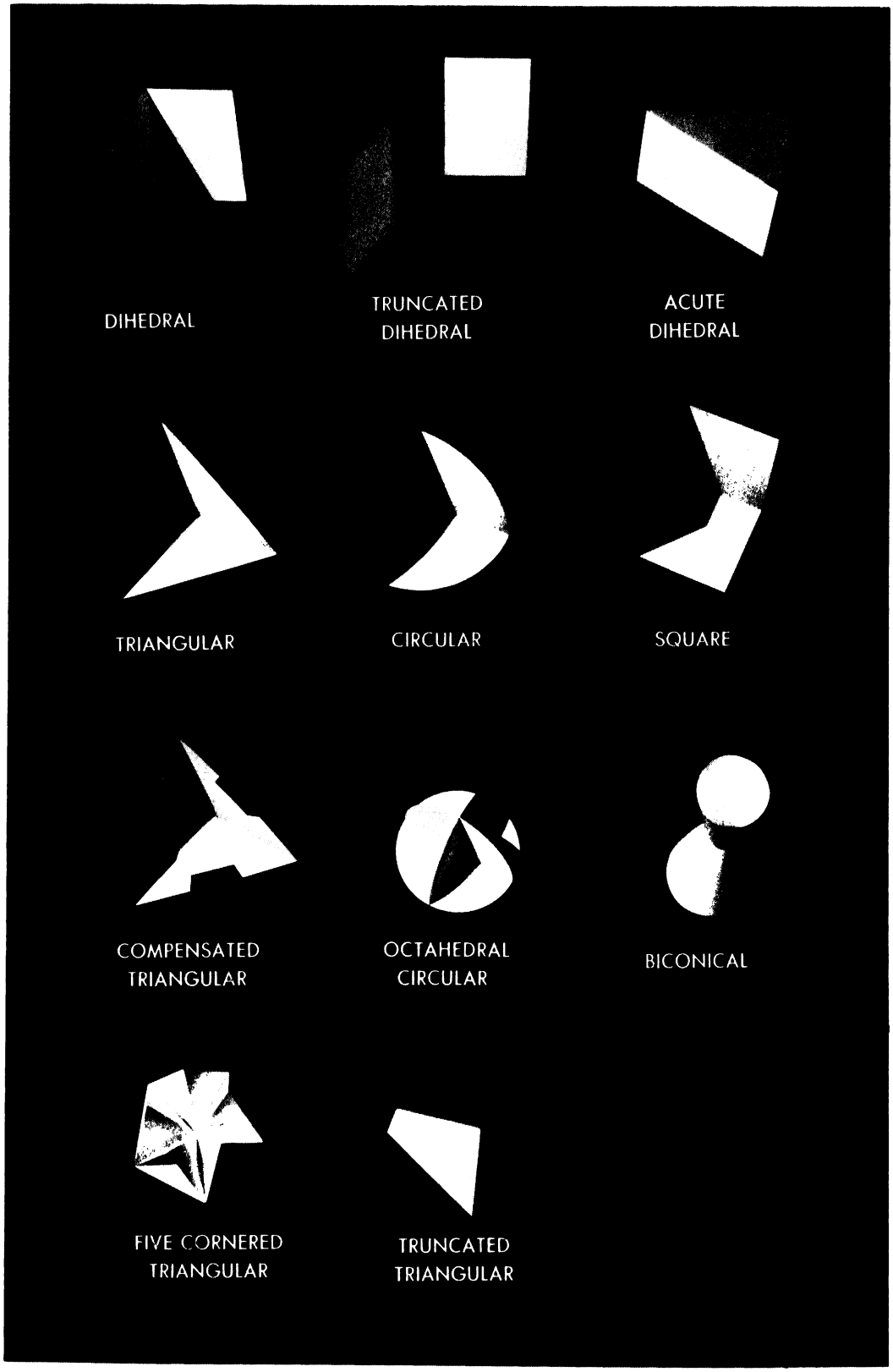

FIG. 1 MULTIPLE SCATTERERS

I

INTRODUCTION AND SUMMARY

If a body is not convex, radiation incident on it may be reflected a number of times from one part of the body to another before finally being reflected away from the body. These multiple reflections have an important effect on the radar cross-section of a complicated body such as an airplane. Therefore, as part of Willow Run Research Center's program of determining radar cross-sections, this study of the radar cross-sections of multiple scatterers at short wavelengths has been made. This paper presents a summary of known data on multiple scatterers, together with a few new formulas for special cases.

The best known and best understood example of a multiple scatterer is the corner reflector, which is widely used as a beacon and as a standard in experimental determinations of cross-section. A corner reflector consists of sections of three mutually orthogonal planes, and has the characteristic property of giving a large monostatic cross-section over a wide range of directions of incidence.*

A simple approximation to the bistatic cross-section of a corner reflector is given in Equations (2.1-5) and (2.1-6). An optical model to be used in conjunction with Eq. (2.1-5) for determining the monostatic cross-section of a corner reflector is described in Section 2.2. Explicit expressions for the monostatic cross-sections of square and triangular corner reflectors are given in Section 2.3. A study of the bistatic cross-section of a square corner reflector with the transmitter on the axis of symmetry is made in Section 2.4. A discussion of the effects of constructional errors, compensation, and truncation is given in Section 2.5.

When the multiple scatterer has surfaces which are curved the cross-section may be obtained by applying Eq.(2.1-4). The application of this formula involves the geometrical optics approximation to the fields on the scattering surface and this is given in Eq.(3.1-1). In the special case when the radii of curvature of the scattering body are finite at all of the reflection points the cross-section may be obtained by using Eq.(3.3-10) and (2.1-3). To illustrate the methods used, the cross-sections of a biconical reflector and of a pair of spheres are obtained Sec. 3.2 and 3.4).

*Certain closely related configurations are also commonly referred to as corner reflectors.

A sampling of experimental data on corner reflectors is quoted in Section IV. The authors wish to express their appreciation for the kind permission of the Bell System Technical Journal to reproduce Figures 17-21, and of Dr. R. D. O'Neal to reproduce Figures 15 and 16 and the figures in the appendix.

II

THE CORNER REFLECTOR*

2.1 Analytical Method for Determining the Radar Cross-Section of the Corner Reflector

Although the simplest method for obtaining radar cross-sections is the method of geometrical optics (References 1 and 2), this method is not directly applicable to corner reflectors because it predicts that the radar cross-section is infinite in the directions in which radiation is specularly reflected and zero elsewhere. More explicitly, for a scattering body consisting only of plane surfaces, geometric optics predicts that the incident radiation is scattered into a region which, at large distances from the body, subtends a vanishingly small solid angle. Actually the radiation must be spread, by diffraction, over a region of solid angle $(\lambda/h)^2$ where λ is the wavelength of the radiation and h is the characteristic dimension of the body. Near the body this objection no longer exists so that geometrical optics can be used to obtain the fields on the surface of the scatterer when $\lambda << h$. When the magnetic field is known on the surface of a perfectly conducting body the following formula (Reference 3, page 466) can be used to obtain the scattered magnetic field at any point in space:

$$\vec{H}_s = \frac{1}{4\pi} \int_S (\hat{n} \times \vec{H}) \times \nabla \frac{e^{ikR'}}{R'} \, dS \qquad (2.1\text{-}1)$$

where $\vec{H}$ is the magnetic field on the surface of integration,
$\vec{H}_s$ is the scattered magnetic field,
$\hat{n}$ is the outward unit normal to the surface,
$k = 2\pi/\lambda$.
R' is the distance between the field point and the integration point.
The integration is to be taken over the entire surface, S, of the body.

When the field point is at a large distance from the body, (2.1-1) can be approximated by

*Much of the material presented in this section appears in Ref. 4.

MISSING
PAGE

where A is the area of the above-mentioned aperture.

The angle, $\delta\psi$, between the beam direction and the direction in which the radar cross-section has decreased by a factor of two is approximately (Ref. 4)

$$\delta\psi = 7.5^{o}\,\lambda/B \qquad \ldots\ldots\ldots \quad (2.1\text{-}6)$$

where B is the radius of gyration of the aperture taken about an axis through the center of gravity of the aperture and perpendicular to the plane in which the deviation from the center of the beam is taken.

2.2 An Optical Model for Corner Reflectors.

One of the beams in which the scattered energy is concentrated is reflected back toward the transmitter. The value of A for this beam determines the monostatic cross-section through (2.1-5). The task of obtaining A analytically can be avoided by use of an optical model which, looked at from any direction, presents an aperture whose projected area is A.

Such an optical model can be constructed by cutting appropriate openings in three mutually orthogonal opaque sheets (Ref. 4 and 5). For the corner reflector in Figure 2, the openings are as shown in Figure 3. Each of the three apertures shown in Figure 3 is obtained by cutting one of the faces of the corner reflector out of each of the four quadrants so as to give a symmetrical figure. Figure 4 shows the optical model consisting of the three apertures of Figure 3. An optical model for any corner reflector can be constructed in precisely the same manner.

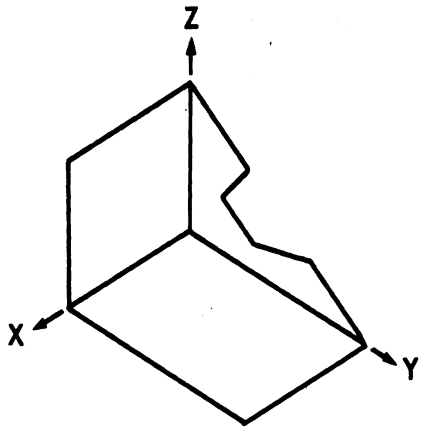

FIG. 2 A CORNER REFLECTOR

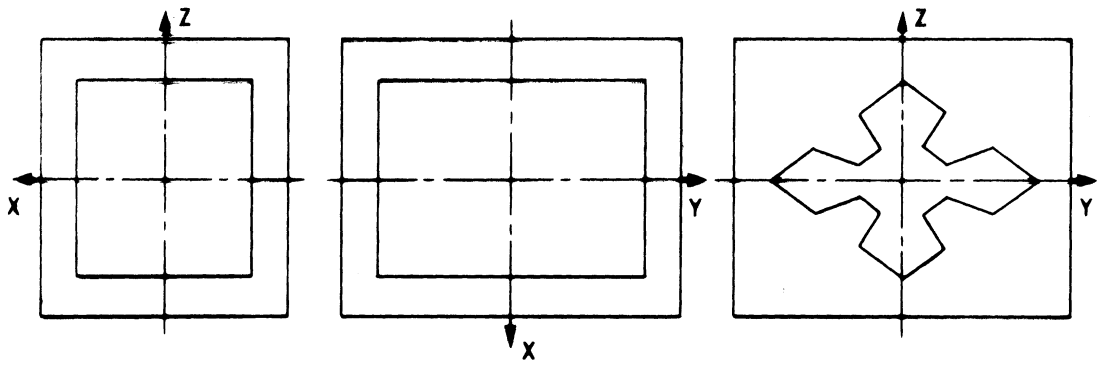

FIG. 3 APERTURES IN OPTICAL MODEL OF CORNER REFLECTOR

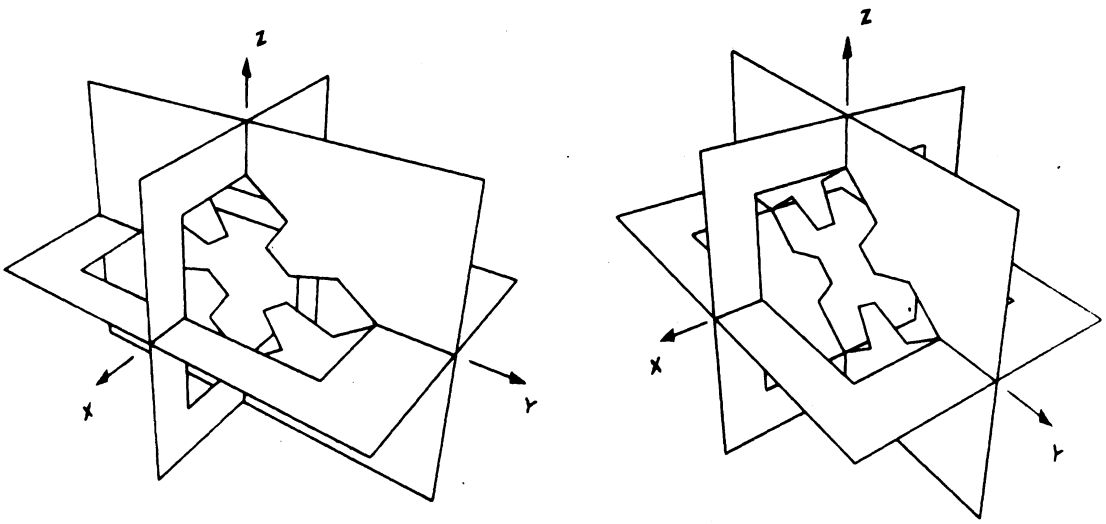

The two views form a stereo pair A three dimensional effect may be obtained by focusing the right eye on the right view, the left eye on the left view, and then superposing the images. Alternatively a standard stereoscopic viewer may be used.

FIG. 4 OPTICAL MODEL OF CORNER REFLECTOR

2.3 Monostatic Cross-Section of Square and Triangular Corner Reflectors.

In Reference 4, the value of A for the beam reflected towards the transmitter has been determined analytically for both square and triangular corner reflectors (Fig. 5).

Square Corner Reflector Triangular Corner Reflector

FIG. 5 SQUARE AND TRIANGULAR CORNER REFLECTORS

The value of A is expressed most simply in terms of the cosines of the angles between the axes of the corner reflector and the direction to the transmitter. If these cosines are $\ell \leq m \leq n$, then A is given by:

For a Square Corner Reflector:

$$A = 4\ell m\, b^2/n \quad , (m \leq n/2)$$

$$A = \ell\left(4 - \frac{n}{m}\right) b^2 \quad , (m \geq n/2) \qquad \ldots\ldots\ldots \quad (2.3\text{-}1)$$

For a Triangular Corner Reflector:

$$A = 4\,\frac{\ell m}{\ell + m + n}\, b^2 \quad , (\ell + m \leq n)$$

$$A = \left(\ell + m + n - \frac{2}{\ell + m + n}\right) b^2 \quad , (\ell + m \geq n) \qquad \ldots\ldots\ldots \quad (2.3\text{-}2)$$

The transmitter direction making equal angles with the three axes is a symmetry axis for square and triangular corner reflectors. If δ is the angle, in degrees, between this symmetry axis and the direction

to the transmitter, then, for small δ , A is given by:

For a Square Corner Reflector:

$$A \simeq \sqrt{3}\ (1-0.0274\,\delta)b^2 \qquad \ldots\ldots\ldots\ldots \quad (2.3\text{-}3)$$

For a Triangular Corner Reflector:

$$A \simeq \left(1/\sqrt{3}\right)(1-0.00076\,\delta^2)b^2 \qquad \ldots\ldots\ldots\ldots \quad (2.3\text{-}4)$$

From these equations and from (2.1-5) it follows that the dimensionless quantity $\sigma\lambda^2/4\pi b^4 = A^2/b^4$ depends only on the direction to the transmitter. Curves of constant A^2/b^4 are plotted in Figure 6 for a square corner reflector using the trilinear coordinates ℓ^2, m^2, and n^2. As can be seen from (2.1-5), (2.3-3), and (2.3-4) the maximum values of σ for square and triangular corner reflectors are $12\pi b^4/\lambda^2$ and $4\pi b^4/3\lambda^2$ respectively.

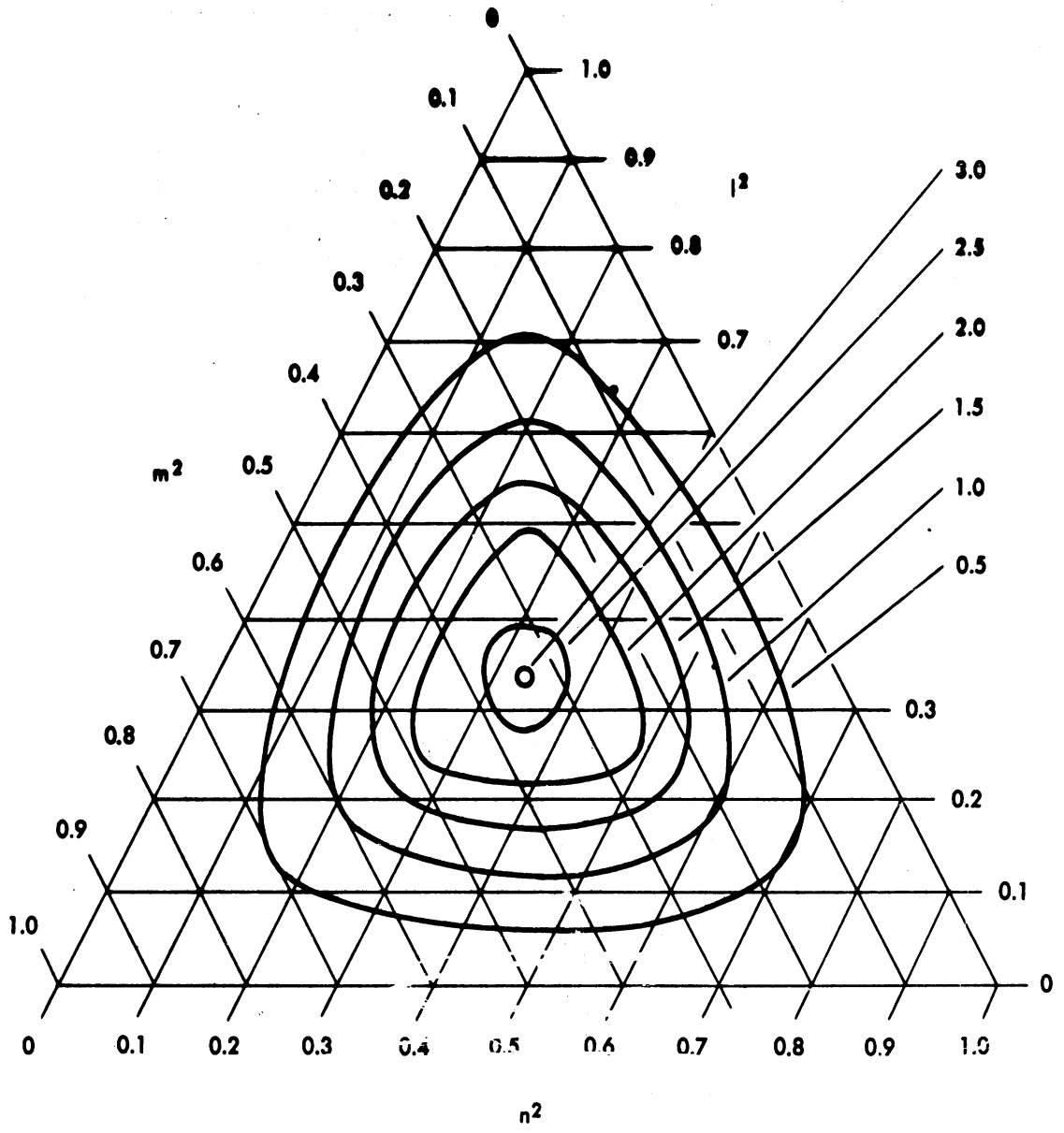

The curves drawn here are for $\frac{\sigma \lambda^2}{4 \pi b^4}$ = constant

FIG. 6 THE MONOSTATIC RADAR CROSS - SECTION OF A SQUARE CORNER REFLECTOR

2.4 Bistatic Cross-Section of a Square Corner Reflector for the Symmetric Case.

The analytic methods described in Section 2.1 are applicable to both the monostatic and bistatic cross-section problems by a suitable choice of the radius vector from the body to the field point. To illustrate the procedure for computing the bistatic cross-section, consider the case of a square corner reflector of side length b. The orientation of the transmitter is as indicated in Figure 7. The receiver is restricted to the first octant ($x \geq 0$, $y \geq 0, z \geq 0$).

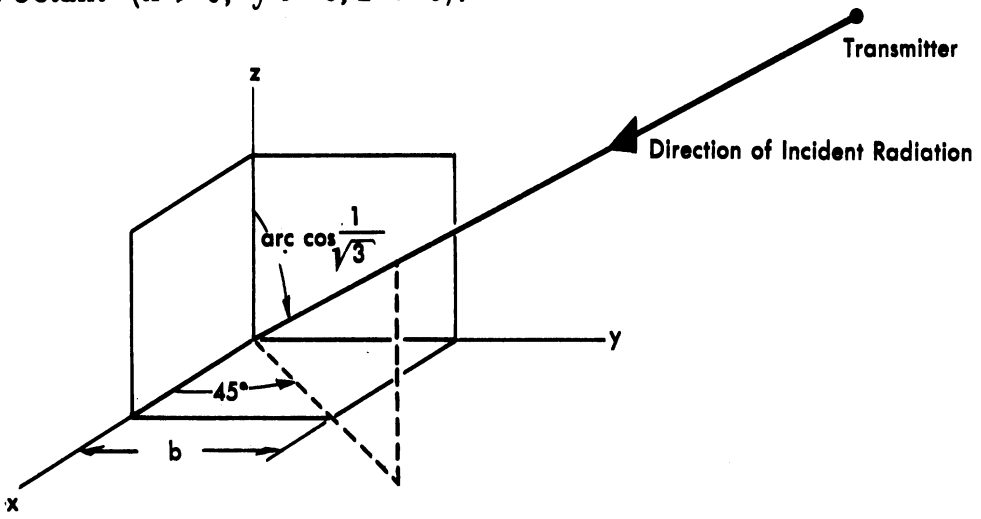

FIG. 7 TRANSMITTER ORIENTATION FOR THE SYMMETRIC BISTATIC CASE

When the wavelength of the incident radiation is less than the side length b, the radar cross-section is determined almost entirely by the triply reflected radiation. Thus, to apply (2.1-1), it is only necessary to obtain the magnetic field, $\vec{H}$, for the triply reflected rays. Consider a ray reflected first from the x-plane, then from the y-plane, and finally from the z-plane, and let the incident magnetic field be

$$\vec{H}_i = \hat{a}\, e^{-i\omega\left(t - \frac{\hat{k}\cdot\vec{r}}{c}\right)} \qquad \text{..... (2.4-1)}$$

where $\hat{a}$ is a unit vector. Suppressing the time factor $e^{-i\omega t}$, the magnetic field along the ray going from the x-plane to the y-plane is

$$\left[\hat{a} - 2(\hat{a}\cdot\hat{i}_x)\hat{i}_x\right] e^{\left\{ ik\left[\hat{k} - 2(\hat{k}\cdot\hat{i}_x)\hat{i}_x\right]\cdot\vec{r}\right\}}, \qquad \text{..... (2.4-2)}$$

where $\hat{i}_x$ is the unit vector in the x direction. The magnetic field along the ray going from the y-plane to the z-plane is

$$\left[-\hat{a} + 2 (\hat{a} \cdot \hat{i}_z) \hat{i}_z \right] e^{\left\{ -ik \left[\hat{k} + 2 (\hat{k} \cdot \hat{i}_z) \hat{i}_z \right] \cdot \vec{r} \right\}} \quad \ldots\ldots\ldots \quad (2.4\text{-}3)$$

On the z-plane $\vec{r} = x\hat{i}_x + y\hat{i}_y$, so that $\hat{i}_z \cdot \vec{r} = 0$. If $\hat{n}$ is a unit vector normal to this surface, then

$$\hat{n} \times \vec{H} = -2 (\hat{i}_z \times \hat{a}) e^{\left\{ -ik \left(\hat{k} \cdot \vec{r} \right) \right\}} \quad \ldots\ldots\ldots \quad (2.4\text{-}4)$$

In general, for triply reflected radiation,

$$\hat{n} \times \vec{H} = -2 (\hat{n} \times \hat{a}) e^{\left\{ -ik \left(\hat{k} \cdot \vec{r} \right) \right\}} \quad \ldots\ldots\ldots \quad (2.4\text{-}5)$$

on the scattering surface.

It is still necessary to determine how much of the corner is illuminated by such triply reflected radiation. A consideration of the optical model shows that the entire corner is illuminated for the transmitter orientation of Figure 7. For orientations of the transmitter other than that in Figure 7, the corner is not entirely illuminated. However, these orientations present no new problems, since the part of the corner that is illuminated in these cases may also be found from the optical model.

From (2.1-4) and (2.4-5) the cross-section of the corner reflector is

$$\sigma = \frac{4\pi}{\lambda^2}\left| \int_0^b \int_0^b (\hat{i}_z \times \hat{a}) \times \hat{R}\, e^{-ik(\hat{k}+\hat{R})\cdot\vec{r}}\, dxdy \right.$$
$$+ \int_0^b \int_0^b (\hat{i}_y \times \hat{a}) \times \hat{R}\, e^{-ik(\hat{k}+\hat{R})\cdot\vec{r}}\, dzdx \qquad (2.4\text{-}6)$$
$$\left. + \int_0^b \int_0^b (\hat{i}_x \times \hat{a}) \times \hat{R}\, e^{-ik(\hat{k}+\hat{R})\cdot\vec{r}}\, dydz \right|^2$$

Let $\hat{R} = R_x \hat{i}_x + R_y \hat{i}_y + R_z \hat{i}_z$, $\hat{k} + \hat{R} = E\hat{i}_x + F\hat{i}_y + G\hat{i}_z$, and $\hat{a} = a_x \hat{i}_x + a_y \hat{i}_y + a_z \hat{i}_z$.

In this notation (2.4-6) becomes

$$\sigma = \frac{4\pi}{\lambda^2}\left| \left[R_z a_x \hat{i}_x + R_z a_y \hat{i}_y - (R_x a_x + R_y a_y)\hat{i}_z \right] \int_0^b \int_0^b e^{-ik(Ex+Fy)}\, dxdy \right.$$
(2.4-7)
$$+ \left[R_x a_y \hat{i}_y + R_x a_z \hat{i}_z - (R_y a_y + R_z a_z)\hat{i}_x \right] \int_0^b \int_0^b e^{-ik(Fy+Gz)}\, dydz$$
$$\left. + \left[R_y a_z \hat{i}_z + R_y a_x \hat{i}_x - (R_z a_z + R_x a_x)\hat{i}_y \right] \int_0^b \int_0^b e^{-ik(Gz+Ex)}\, dzdx \right|^2$$

After performing the integration, (2.4-7) becomes

$$\sigma = \frac{\lambda^2}{4\pi^3}\left|\left[R_z a_x \hat{i}_x + R_z a_y \hat{i}_y - (R_x a_x + R_y a_y)\hat{i}_z\right]\frac{e^{-ikb(E+F)} - e^{-ikbE} - e^{-ikbF} + 1}{EF}\right.$$

$$+\left[R_x a_y \hat{i}_y + R_x a_z \hat{i}_z - (R_y a_y + R_z a_z)\hat{i}_x\right]\frac{e^{-ikb(F+G)} - e^{-ikbG} - e^{-ikbE} + 1}{FG} \qquad (2.4\text{-}8)$$

$$\left.+\left[R_y a_z \hat{i}_z + R_y a_x \hat{i}_x - (R_z a_z + R_x a_x)\hat{i}_y\right]\frac{e^{-ikb(G+E)} - e^{-ikbG} - e^{-ikbE} + 1}{GE}\right|^2$$

To simplify (2.4-8), the following condensation symbols are introduced.

$$c_1 = \frac{\cos kb(F+G) - \cos kbF - \cos kbG - 1}{FG},$$

$$c_2 = \frac{\cos kb(G+E) - \cos kbG - \cos kbE - 1}{GE}, \qquad (2.4\text{-}9)$$

$$c_3 = \frac{\cos kb(E+F) - \cos kbE - \cos kbF - 1}{EF},$$

$$s_1 = \frac{\sin kb(F+G) - \sin kbF - \sin kbG}{FG},$$

$$s_2 = \frac{\sin kb(G+E) - \sin kbG - \sin kbE}{GE},$$

$$s_3 = \frac{\sin kb(E+F) - \sin kbE - \sin kbF}{EF}.$$

In this notation, the radar cross-section of the square corner reflector for the symmetric case is given by

$$\sigma = \frac{\lambda^2}{4\pi^3}\left\{\left[-(R_y a_y + R_z a_z)\, c_1 + R_y a_x c_2 + R_z a_x c_3\right]^2\right.$$
$$+\left[R_x a_y c_1 - (R_x a_x + R_z a_z)\, c_2 + R_z a_y c_3\right]^2$$
$$+\left[R_x a_z c_1 + R_y a_z c_2 - (R_x a_x + R_y a_y)\, c_3\right]^2$$
$$+\left[-(R_y a_y + R_z a_z)\, s_1 + R_y a_x s_2 + R_z a_x s_3\right]^2 \qquad (2.4\text{-}10)$$
$$+\left[R_x a_y s_1 - (R_x a_x + R_z a_z)\, s_2 + R_z a_y s_3\right]^2$$
$$\left.+\left[R_x a_z s_1 + R_y a_z s_2 - (R_x a_x + R_y a_y)\, s_3\right]^2\right\}.$$

This formula gives the radar cross-section for any polarization of the incident electromagnetic wave. To show how the bistatic radar cross-section varies as a function of receiver position for this symmetric case, (2.4-10) has been plotted in Figures 9, 10, 11, and 12 for a corner reflector of side length b = 25 cm., for three values of wavelength, and for the incident magnetic field vector parallel to one of the coordinate surfaces, that is $\hat{a}_H = -\frac{\hat{i}_x}{\sqrt{2}} + \frac{\hat{i}_y}{\sqrt{2}}$

The polar angles designating receiver position are indicated in Figure 8.

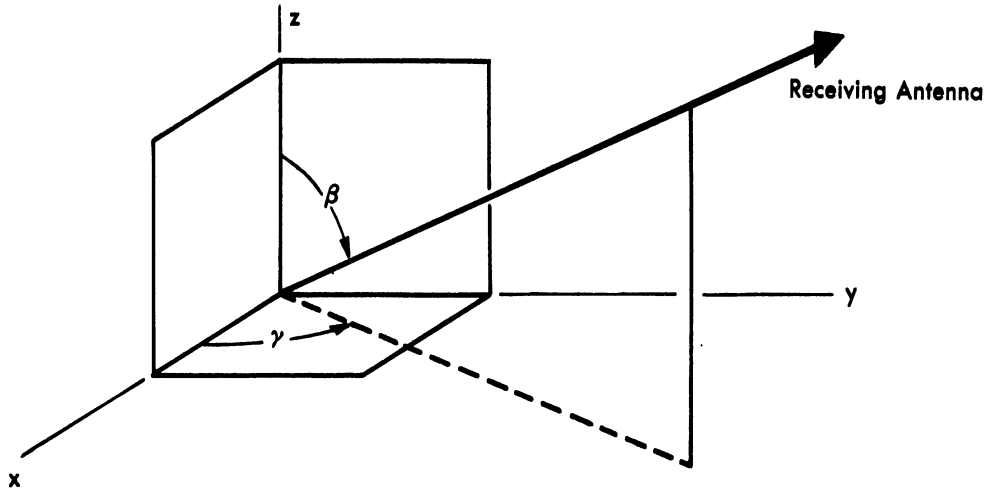

FIG. 8 POLAR ANGLES β AND γ DESCRIBING RECEIVER POSITION

Figure 9 shows the variation of σ with γ for $\beta = 54.74^{\circ}$ and for wavelengths of 3, 10, and 30 cm. The variation of σ with β for a wavelength of 3 cm. and $\gamma = 15^{\circ}$, 30°, and 45° is shown in Figure 10. The $\gamma = 45^{\circ}$ values were obtained at two degree intervals while the $\gamma = 15^{\circ}$ and $\gamma = 30^{\circ}$ values were obtained at 10 degree intervals. Because the 10° interval is too large to show the variation of σ with β accurately, curves have not been drawn for a wavelength of 10 cm. Figures 11 and 12 show the variation of σ with β for $\gamma = 45^{\circ}$ and wavelengths of 10 and 30 cm. respectively.

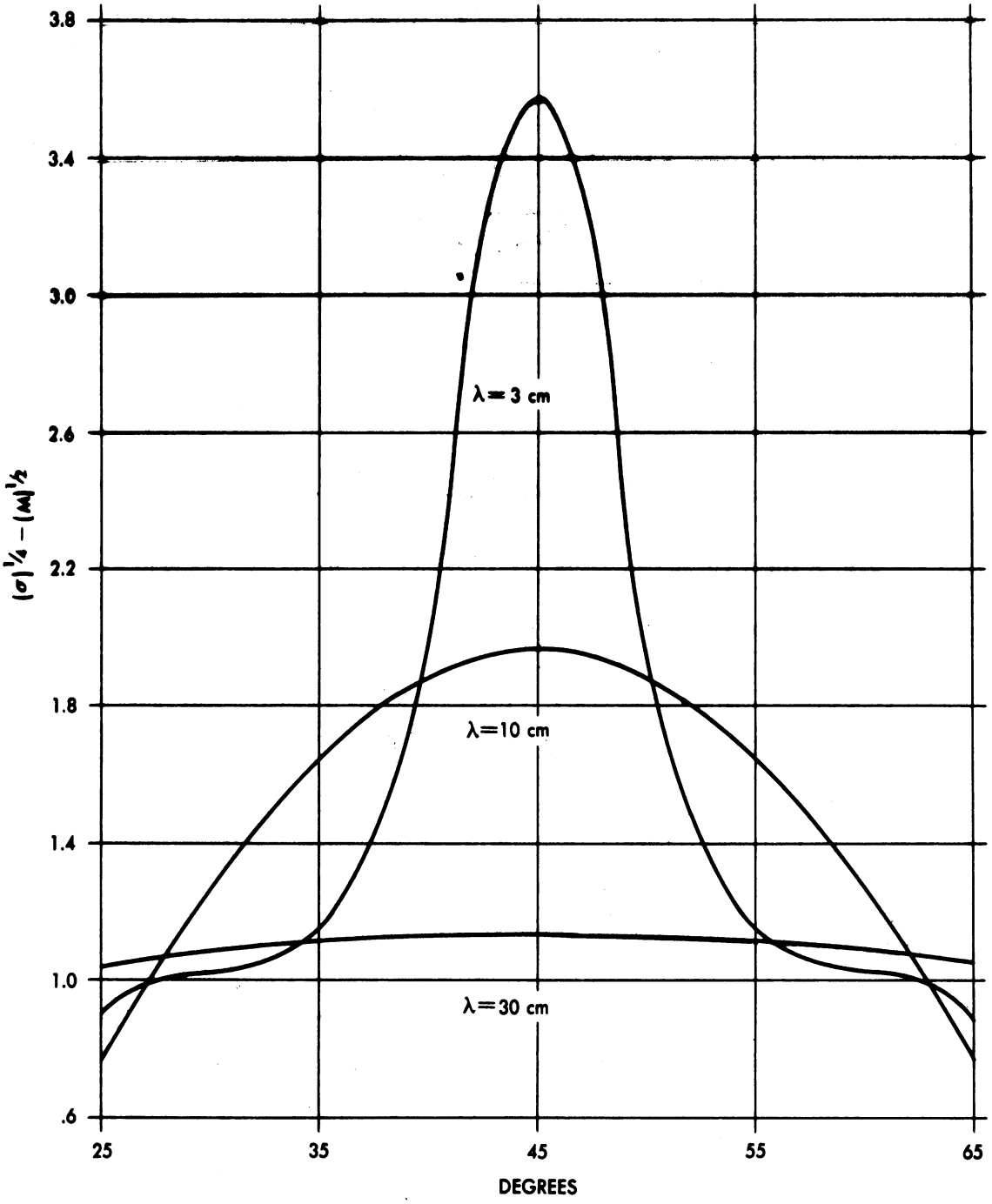

FIG. 9 BISTATIC RADAR CROSS - SECTION OF A SQUARE CORNER REFLECTOR AS A FUNCTION OF γ

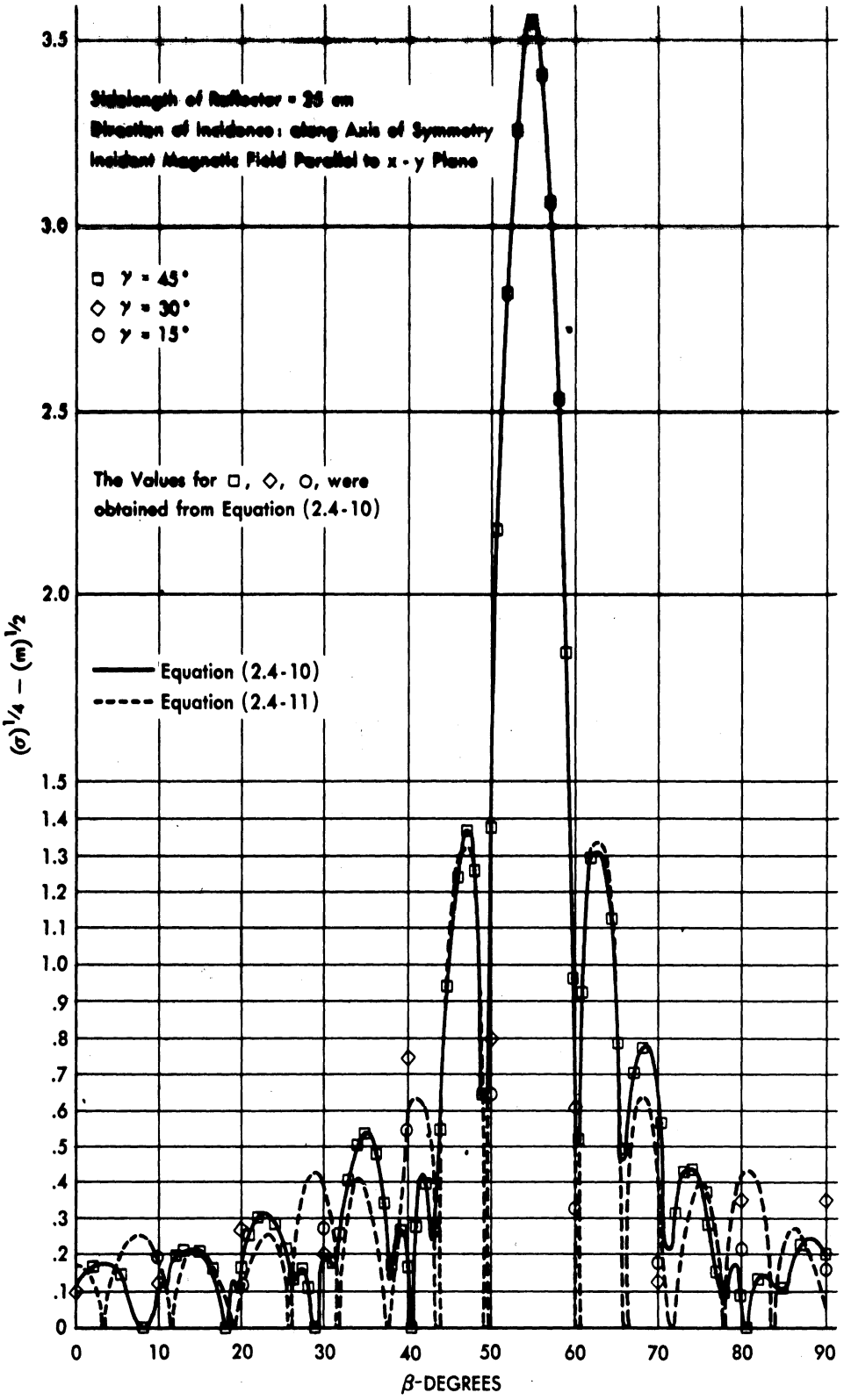

FIG. 10 BISTATIC RADAR CROSS-SECTION OF A SQUARE CORNER REFLECTOR AS A FUNCTION OF β FOR A WAVELENGTH OF 3 CM

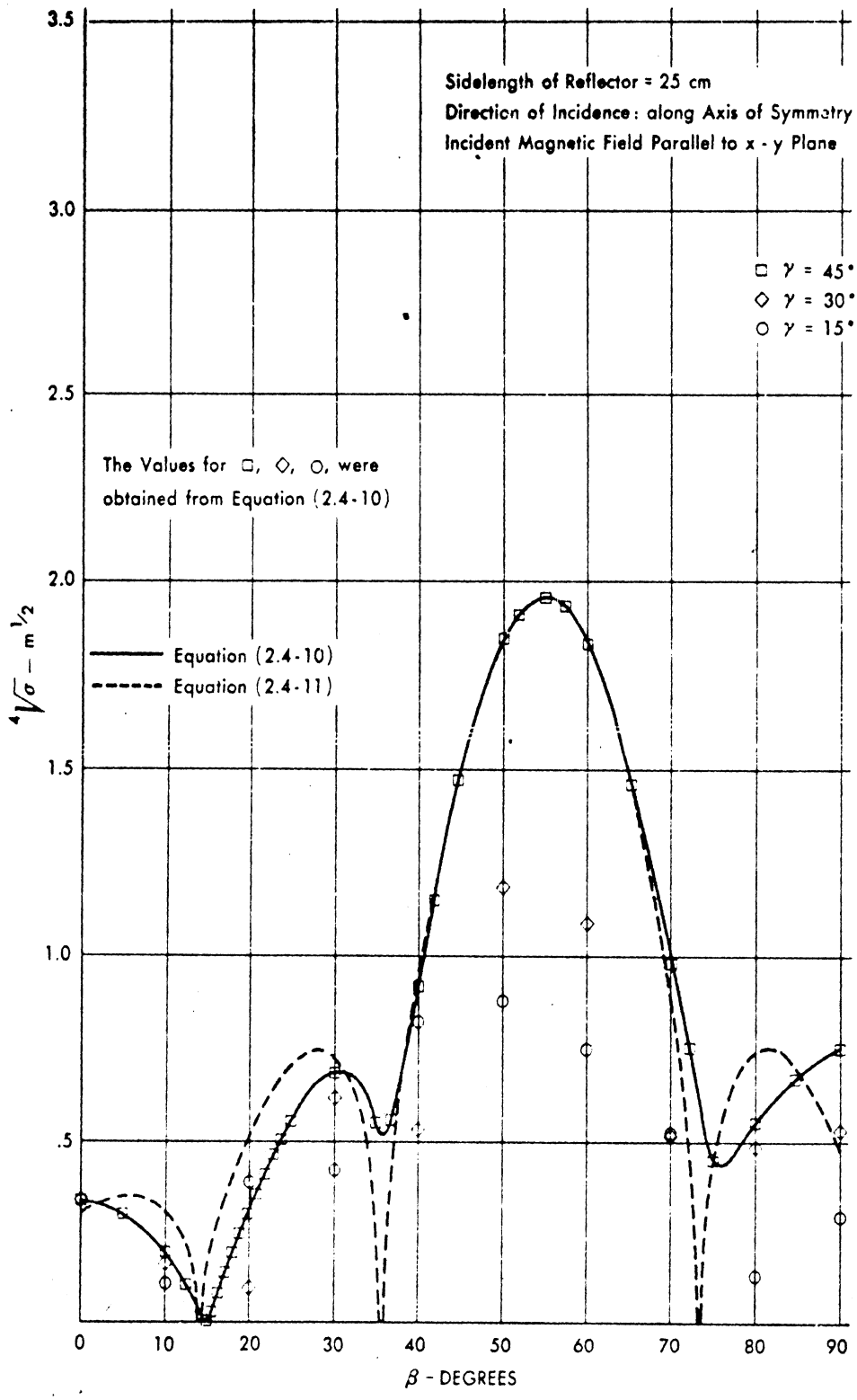

FIG. 11 BISTATIC RADAR CROSS-SECTION OF A SQUARE CORNER REFLECTOR AS A FUNCTION OF β FOR A WAVELENGTH OF 10 CM

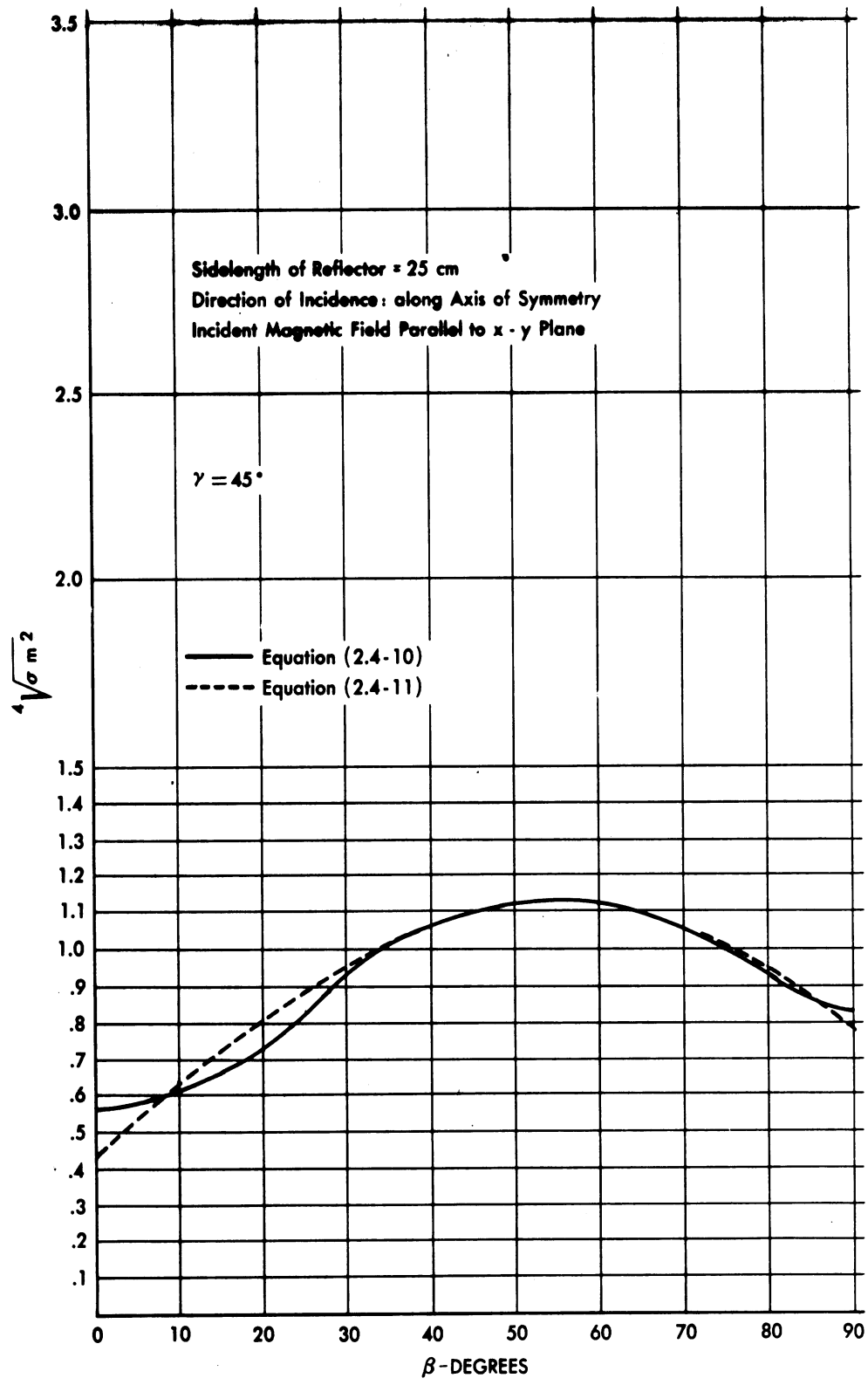

FIG. 12 BISTATIC RADAR CROSS-SECTION OF A SQUARE CORNER REFLECTOR AS A FUNCTION OF β FOR A WAVELENGTH OF 30 CM

As was noted in section 2.1, the scattering pattern of a corner reflector is approximately the same as the diffraction pattern of an equivalent aperture. For the symmetric case considered, the diffracting aperture is hexagonal. For $\gamma = 45^{\circ}$, the bistatic radar cross-section for this aperture is

$$\sigma = \frac{108\pi b^4}{\lambda^2 \tau^4} (\sin\tau \sin\tau/3)^2 \qquad (2.4\text{-}11)$$

where $$\tau = \frac{\pi b}{\lambda}\left[\frac{1}{\sqrt{2}} \sin\beta - \cos\beta\right] .$$

The values of radar cross-section (2.4-11) as predicted by this equivalent aperture are also plotted in Figures 10, 11, and 12 for comparison with the values obtained from (2.4-10). It should be noted that the half-power widths given by both (2.4-10) and (2.4-11) agree with the values predicted by (2.1-6).

Although the geometric optics and physical optics approximations are based on the assumption that the wavelength is small compared to the characteristic dimension of the body, there is reason to believe that the error introduced by the use of these approximation techniques when b/λ is approximately one is sometimes much less than an order of magnitude. Kouyoumjian (Ref. 6), for example, has found that the monostatic radar cross-section predicted by physical optics for a flat plate at normal incidence does not deviate from the exact electromagnetic solution by more than a factor of five for the range b/λ between 0.8 and 5. Since it is not likely that exact computations will be made of the cross-section of corner reflectors in the near future, and since there is reason to believe that the approximation techniques do yield order of magnitude answers for the square corner reflector for $\lambda \approx b$, these techniques have been applied for a wavelength of 30 cm. (i.e. $\lambda/b = 1.2$).

2.5 Effect of Constructional Errors, Compensation, and Truncation.

Corner reflectors are generally used to direct a large signal back toward the transmitter. This large signal is reduced in intensity if the corner is not perfectly constructed. If the faces of a corner reflector do not meet at exactly 90° then the beam which would have been reflected back to the transmitter is divided into several beams, none of which, in general, are directed exactly toward the transmitter. As a result, there will be a reduction in signal received at the transmitter. In Reference 4 the magnitudes of the errors which reduce the signal returned by square or triangular corners (Fig. 5) to one half the maximum returned signal are calculated. This error, Δ , is determined as follows: if one of the faces of the corner is rotated about one of the coordinate axes through which it passes, then Δ is the distance which the part of the face farthest from the axis moves. These errors are independent of the size of the corner, and therefore are difficult to avoid for large corners and small wave lengths. For incidence along the axis of symmetry these errors are

Square Corner: one error, $\Delta = .40\lambda$
three equal errors, $\Delta = .24\lambda$

Triangular Corner: one error, $\Delta = .70\lambda$
three equal errors, $\Delta = .35\lambda$

For some applications, such as a movable corner used as a beacon, it is desirable to sacrifice some of the strength of the returned signal in order to obtain a usable signal over a wider range of incidence angles on the corner. This flattening and widening of the monostatic response pattern can be accomplished by truncation or compensation (Ref. 5), i.e., the removal of some of the reflecting surface (see Sec. 4).

III

OTHER MULTIPLE SCATTERERS

3.1 Formulas for Scattering from Curved Surfaces: Fock's Method.

In Section II only scattering from surfaces having infinite radii of curvature was considered. In this section multiple scattering from surfaces having finite radii of curvature will be considered. In Reference 7, formulas are developed for the scattering from curved surfaces. These formulas, which are useful for computing the cross-section of bodies with curved surfaces, are summarized in this section.

The scattered electric and magnetic fields, as given by geometric optics, are

$$\vec{E}_s = \left[\vec{E}_i - 2\hat{n} \times (\vec{E}_i \times \hat{n}) \right] \sqrt{\frac{D(0)}{D(R)}} \; e^{ikR} , \tag{3.1-1}$$

$$\vec{H}_s = \left[\vec{H}_i - 2 (\hat{n} \cdot \vec{H}_i) \hat{n} \right] \sqrt{\frac{D(0)}{D(R)}} \; e^{ikR}$$

where D(R) is the cross-sectional area of a bundle of rays at a distance R from the specular reflection point, and $\vec{E}_i$, $\vec{H}_i$ is the incident field at the specular reflection point.

The area of the bundle of rays at a distance R is given by

$$D(R) = \begin{vmatrix} T^u_u & T^u_v \\ T^v_u & T^v_v \end{vmatrix} \tag{3.1-2}$$

where T^p_q is the symmetrical tensor

$$T^{p}_{q} = g^{pu} T_{uq} + g^{pv} T_{vq} \qquad (3.1\text{-}3)$$

and

$$T_{pq} = g_{pq} - \Omega_{p} \Omega_{q} + R (\Omega_{pq} - \cos\zeta\, G_{pq}) . \qquad (3.1\text{-}4)$$

Here u and v are curvilinear coordinates on the scattering surface and g_{pq} is the metric tensor given by

$$d\sigma^{2} = g_{uu}\, du^{2} + 2g_{uv}\, du\, dv + g_{vv}\, dv^{2} \qquad (3.1\text{-}5)$$

where $d\sigma$ is an element of arc on the surface. The g^{pq} that appear in (3.1-3) are related to the g_{pq} by

$$\begin{bmatrix} g^{uu} & g^{uv} \\ g^{vu} & g^{vv} \end{bmatrix} = \frac{1}{g_{uu} g_{vv} - g_{uv}^{2}} \begin{bmatrix} g_{vv} & -g_{uv} \\ -g_{vu} & g_{uu} \end{bmatrix} . \qquad (3.1\text{-}6)$$

G_{pq} is the curvature tensor of the surface given by

$$-G_{pq} = \frac{\partial n_{x}}{\partial p} \frac{\partial x}{\partial q} + \frac{\partial n_{y}}{\partial p} \frac{\partial y}{\partial q} + \frac{\partial n_{z}}{\partial p} \frac{\partial z}{\partial q} \qquad (3.1\text{-}7)$$

where n_{x}, n_{y}, and n_{z} are the components of the unit normal to the surface at a point x, y, z of the surface. The angle ζ is the angle between the direction of incidence and the normal to the surface. Ω is defined in terms of the phase of the incident wave on the scattering surface $e^{ik\Omega(u,v)}$. Ω_{p} is the ordinary derivative of Ω with respect to p.

$$\Omega_p = \frac{\partial \Omega}{\partial p} . \qquad (3.1\text{-}8)$$

Ω_{pq} is the second covariant derivative

$$\Omega_{pq} = \frac{\partial^2 \Omega}{\partial p \partial q} - \left\lceil^{u}_{pq} \frac{\partial \Omega}{\partial u} - \left\lceil^{v}_{pq} \frac{\partial \Omega}{\partial v} \right. \right. . \qquad (3.1\text{-}9)$$

$\left\lceil^{p}_{qw}\right.$ is the Christoffel symbol of the second kind,

$$\left\lceil^{p}_{qw}\right. = g^{pu} \left[q, w; u\right] + g^{pv} \left[q, w; v\right] \qquad (3.1\text{-}10)$$

and [p,q;w] is the Christoffel symbol of the first kind

$$\left[p, q; w\right] = \frac{1}{2}\left(\frac{\partial g_{pw}}{\partial q} + \frac{\partial g_{qw}}{\partial p} - \frac{\partial g_{pq}}{\partial w}\right) . \qquad (3.1\text{-}11)$$

3.2 Scattering from Two Spheres

As an example of the application of the formulas in Section 3.1, consider the back-scattering from two spheres of equal radius for an electric field $\hat{i}_x e^{-ikz}$ incident perpendicular to the common axis of the spheres.

(Positive x-axis points into the paper)

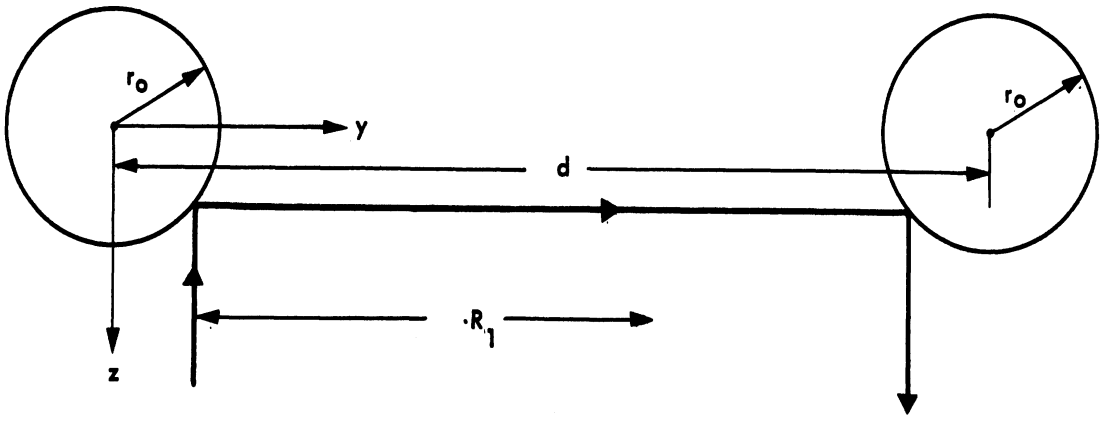

FIG. 13 REFLECTION GEOMETRY FOR TWO SPHERES

First, consider the doubly reflected ray shown in Figure 13. For the reflection from the first sphere the coordinates u and v are

$$u_1 = \Theta_1 ,$$
$$v_1 = \phi_1 \qquad (3.2\text{-}1)$$

where Θ_1 and ϕ_1 are related to the Cartesian coordinates by

$$x = r_o \sin\Theta_1 \cos\phi_1 ,$$
$$y = r_o \sin\Theta_1 \sin\phi_1 , \qquad (3.2\text{-}2)$$
$$z = r_o \cos\Theta_1 .$$

The normal on the surface of the sphere is

$$\hat{n} = \sin\Theta_1 \cos\phi_1 \hat{i}_x + \sin\Theta_1 \sin\phi_1 \hat{i}_y + \cos\Theta_1 \hat{i}_z . \qquad (3.2\text{-}3)$$

Thus, by (3.1-7)

$$-\begin{bmatrix} G_{\Theta_1\Theta_1} & G_{\Theta_1\phi_1} \\ G_{\phi_1\Theta_1} & G_{\phi_1\phi_1} \end{bmatrix} = \begin{bmatrix} r_o & 0 \\ 0 & r_o \sin^2\Theta_1 \end{bmatrix} \qquad (3.2\text{-}4)$$

The square of the element of arc on the sphere is

$$d\sigma^2 = r_o^2\, d\theta_1^2 + r_o^2 \sin^2\theta_1\, d\phi_1^2 \qquad (3.2\text{-}5)$$

so that

$$\begin{bmatrix} g_{\theta_1\theta_1} & g_{\theta_1\phi_1} \\ g_{\phi_1\theta_1} & g_{\phi_1\phi_1} \end{bmatrix} = \begin{bmatrix} r_o^2 & 0 \\ 0 & r_o^2 \sin^2\theta_1 \end{bmatrix} \qquad (3.2\text{-}6)$$

and

$$\begin{bmatrix} g^{\theta_1\theta_1} & g^{\theta_1\phi_1} \\ g^{\phi_1\theta_1} & g^{\phi_1\phi_1} \end{bmatrix} = \begin{bmatrix} \frac{1}{r_o^2} & 0 \\ 0 & \frac{1}{r_o^2 \sin^2\theta_1} \end{bmatrix} \qquad (3.2\text{-}7)$$

The phase factor is

$$\Omega_1(\theta_1, \phi_1) = -z = -r_o \cos\theta_1 \qquad (3.2\text{-}8)$$

and the first derivatives of the phase factor are

$$\begin{aligned} \Omega_{1\theta_1} &= r_o \sin\theta_1 , \\ \Omega_{1\phi_1} &= 0 . \end{aligned} \qquad (3.2\text{-}9)$$

The Christoffel symbols of the first kind are

$$\begin{aligned} \left[\phi_1, \phi_1; \theta_1\right] &= -r_o^2 \sin\theta_1 \cos\theta_1 , \\ \left[\phi_1, \theta_1; \phi_1\right] &= r_o^2 \sin\theta_1 \cos\theta_1 , \end{aligned} \qquad (3.2\text{-}10)$$

$$\left[\theta_1, \theta_1; \theta_1\right] = \left[\theta_1, \theta_1; \phi_1\right] = \left[\theta_1, \phi_1; \theta_1\right] = \left[\phi_1, \phi_1; \phi_1\right] = 0 .$$

The Christoffel symbols of the second kind are

$$\left[\begin{matrix}\theta_1\\ \phi_1\phi_1\end{matrix}\right] = -\sin\theta_1\cos\theta_1 \quad ,$$

$$\left[\begin{matrix}\phi_1\\ \phi_1\theta_1\end{matrix}\right] = \cot\theta_1 \quad , \qquad (3.2\text{-}11)$$

$$\left[\begin{matrix}\theta_1\\ \theta_1\theta_1\end{matrix}\right] = \left[\begin{matrix}\phi_1\\ \theta_1\theta_1\end{matrix}\right] = \left[\begin{matrix}\theta_1\\ \theta_1\phi_1\end{matrix}\right] = \left[\begin{matrix}\phi_1\\ \phi_1\phi_1\end{matrix}\right] = 0 \quad .$$

Therefore, by (3.1-9) the second covariant derivatives are

$$\begin{bmatrix} \Omega_{1\theta_1\theta_1} & \Omega_{1\theta_1\phi_1} \\ \Omega_{1\phi_1\theta_1} & \Omega_{1\phi_1\phi_1} \end{bmatrix} = \begin{bmatrix} -\Omega_1 & 0 \\ 0 & -\Omega_1\sin^2\theta_1 \end{bmatrix} \quad . \qquad (3.2\text{-}12)$$

Since $\zeta_1 = \theta_1$, and $\Omega_1 = -r_o\cos\theta_1$ the symmetric tensor (3.1-4) is

$$\begin{bmatrix} T_{\theta_1\theta_1} & T_{\theta_1\phi_1} \\ T_{\phi_1\theta_1} & T_{\phi_1\phi_1} \end{bmatrix} = \begin{bmatrix} \Omega_1^2 - 2R_1\Omega_1 & 0 \\ 0 & (r_o^2-\Omega_1^2)\left(1-2\dfrac{R_1\Omega_1}{r_o^2}\right) \end{bmatrix} \quad . \qquad (3.2\text{-}13)$$

The cross-sectional area of a bundle of rays at a distance R_1 from the specular reflection point is

$$D_1(R_1) = \begin{vmatrix} T_{\theta_1}^{\theta_1} & T_{\phi_1}^{\theta_1} \\ T_{\theta_1}^{\phi_1} & T_{\phi_1}^{\phi_1} \end{vmatrix} = \begin{vmatrix} \dfrac{\Omega_1^2 - 2R_1\Omega_1}{r_o^2} & 0 \\ 0 & 1-\dfrac{2R_1\Omega_1}{r_o^2} \end{vmatrix} \qquad (3.2\text{-}14)$$

$$= \cos\theta_1\left(\cos\theta_1 + \frac{2R_1}{r_o}\right)\left(1 + 2\frac{R_1}{r_o}\cos\theta_1\right) \quad .$$

The electric field (3.1-1) scattered from the first sphere is

$$-\hat{i}_x \sqrt{\frac{\cos\Theta_1}{(\cos\Theta_1 + 2\frac{R_1}{r_o})(1 + 2\frac{R_1}{r_o}\cos\Theta_1)}}\, e^{ik(R_1 - r_o\cos\Theta_1)} \quad . \tag{3.2-15}$$

For the ray shown in Figure 13, $\Theta_1 = \pi/4$ so that the electric field incident on the second sphere is

$$\frac{-\hat{i}_x\, e^{ik\left(d - \frac{3}{\sqrt{2}} r_o\right)}}{\sqrt{(2\sqrt{2}\,\frac{d}{r_o} - 3)(\sqrt{2}\,\frac{d}{r_o} - 1)}} \quad . \tag{3.2-16}$$

On the second sphere the coordinates u and v are taken to be $u_2 = \Theta_2$ and $v_2 = \phi_2$. These coordinates are related to the Cartesian coordinates by

$$\begin{aligned} x &= r_o \sin\Theta_2 \cos\phi_2 \quad , \\ y &= d + r_o \sin\Theta_2 \sin\phi_2 \quad , \\ z &= r_o \cos\Theta_2 \quad . \end{aligned} \tag{3.2-17}$$

The metric and curvature tensors, and the Christoffel symbols, for the second sphere are obtained from those of the first sphere by replacing Θ_1 and ϕ_1 by Θ_2 and ϕ_2.

The phase function on the second sphere is given by the simultaneous equations

$$(\Omega_2 - \Omega_1)\sin 2\theta_1 \cos\phi_1 = r_o \sin\theta_2 \cos\phi_2 - r_o \sin\theta_1 \cos\phi_1 ,$$

$$(\Omega_2 - \Omega_1)\sin 2\theta_1 \sin\phi_1 = d + r_o \sin\theta_2 \sin\phi_2 - r_o \sin\theta_1 \sin\phi_1, \quad (3.2\text{-}18)$$

$$(\Omega_2 - \Omega_1)\cos 2\theta_1 = r_o \cos\theta_2 - r_o \cos\theta_1 ,$$

where in this example $\theta_1 = \theta_2 = \frac{\pi}{4}$, $\phi_1 = \frac{\pi}{2}$, and $\phi_2 = \frac{3\pi}{2}$.

Hence, the phase factor and its derivatives for this example are

$$\Omega_2 = d - \frac{3}{\sqrt{2}} r_o ,$$

$$\Omega_{2\theta_2} = -\frac{r_o}{\sqrt{2}} ; \Omega_{2\phi_2} = 0 , \quad (3.2\text{-}19)$$

$$\Omega_{2\theta_2\theta_2} = \frac{2d - \frac{r_o}{\sqrt{2}}}{2\sqrt{2}\,\frac{d}{r_o} - 3}, \Omega_{2\phi_2\phi_2} = \frac{\frac{d}{2} + \frac{r_o}{2\sqrt{2}}}{\sqrt{2}\,\frac{d}{r_o} - 1}, \Omega_{2\theta_2\phi_2} = 0 .$$

The metric and curvature tensors at $\theta_2 = \pi/4$ and $\phi_2 = 3\pi/2$ are

$$\begin{bmatrix} g_{\theta_2\theta_2} & g_{\theta_2\phi_2} \\ g_{\phi_2\theta_2} & g_{\phi_2\phi_2} \end{bmatrix} = \begin{bmatrix} r_o^2 & 0 \\ 0 & \frac{r_o^2}{2} \end{bmatrix} \quad (3.2\text{-}20)$$

and

$$\begin{bmatrix} G_{\theta_2\theta_2} & G_{\theta_2\phi_2} \\ G_{\phi_2\theta_2} & G_{\phi_2\phi_2} \end{bmatrix} = \begin{bmatrix} -r_o & 0 \\ 0 & -\frac{r_o}{2} \end{bmatrix} . \qquad (3.2\text{-}21)$$

Since $\zeta_2 = \pi/4$, the symmetrical tensor (3.1-4) is

$$\begin{bmatrix} T_{\theta_2\theta_2} & T_{\theta_2\phi_2} \\ T_{\phi_2\theta_2} & T_{\phi_2\phi_2} \end{bmatrix} = \begin{bmatrix} \frac{r_o^2}{2} + \frac{4d - 2\sqrt{2}\, r_o}{2\sqrt{2}\, d - 3\, r_o} - r_o R_2 & 0 \\ 0 & \frac{r_o^2}{2} + \frac{d r_o R_2}{\sqrt{2}\, d - r_o} \end{bmatrix} . \qquad (3.2\text{-}22)$$

The cross-sectional area of the bundle of rays at a distance R_2 from the specular reflection point is

$$D_2(R_2) = \left(\frac{1}{2} + \frac{R_2}{r_o} \frac{4d - 2\sqrt{2}\, r_o}{2\sqrt{2}\, d - 3 r_o} \right) \left(1 + \frac{R_2}{r_o} \frac{2d}{\sqrt{2}\, d - r_o} \right) . \qquad (3.2\text{-}23)$$

Therefore, at a large distance from the scatterer, for the doubly reflected ray shown in Figure 13, the scattered electric field is

$$\frac{r_o^2\, e^{ik(z + d - 2\sqrt{2}\, r_o)}}{4\, dz \sqrt{1 - \frac{r_o}{\sqrt{2}\, d}}} \hat{i}_x . \qquad (3.2\text{-}24)$$

There is a second doubly reflected ray which gives a contribution equal to (3.2-24) and there are two singly reflected rays each of which contribute to the back scattered electric field by an amount

$$-\frac{r_o}{2z} e^{ik(z - 2r_o)} \hat{i}_x \,. \tag{3.2-25}$$

In addition there are back-scattered rays which are reflected more than twice. If the distance between the centers of the spheres is much larger than the radii of the spheres, the radiation which undergoes more than two reflections may be neglected and the total reflected field is approximately

$$\left[-r_o e^{-2ikr_o} + \frac{r_o^2 e^{ik(d - 2\sqrt{2}\, r_o)}}{2d\sqrt{1 - \frac{r_o}{\sqrt{2}d}}} \right] \frac{e^{ikz}}{z} \hat{i}_x \,. \tag{3.2-26}$$

3.3 Formulas for Scattering From Curved Surfaces: The Method of Stationary Phase.

Another technique for finding the scattered fields when the wavelength is less than a characteristic dimension of the scatterer is the method of stationary phase. The field associated with a multiply reflected ray, as given by this method, depends upon the radii of curvature of the body at the specular reflection points. These radii of curvature are assumed to be finite.

A Cartesian coordinate system is used at each reflection point. The z-axis is taken along the normal to the surface, and the x- and y-axes are chosen so that the x and y planes are the principal sections of the surface, that is sections in which the principle radii of curvature are obtained. In the vicinity of the reflection points the equations of the surfaces are, approximately,

$$z_j = -\frac{x_j^2}{2\rho_{j1}} - \frac{y_j^2}{2\rho_{j2}} \qquad (j = 1, 2, 3, \ldots, N) \qquad (3.3\text{-}1)$$

where ρ_{j1} and ρ_{j2} are the principle radii of curvature of the j'th surface. Let Θ_j and ϕ_j represent the polar angles at the j'th reflection point, $\vec{r}_j$ represent the radius vector to a point on the j'th surface from a fixed arbitrary reference point. Assume the incident magnetic field to be $\hat{a}e^{ik(\hat{k}\cdot\vec{R})}$ where $\vec{R}$ is the radius vector from the reference point to an arbitrary point in space. From equation (2.1-1) the field scattered from the first surface is

$$\vec{H}_s = \frac{1}{2\pi}\int(\hat{n}_1 \times \hat{a}) \times \nabla \frac{e^{ik\left|\vec{R}-\vec{r}_1\right|}}{\left|\vec{R}-\vec{r}_1\right|} e^{ik\hat{k}\cdot\vec{r}_1}\, ds_1 \qquad (3.3\text{-}2)$$

and the multiply scattered field reflected from the N surfaces in succession is

$$\vec{H}_s = \frac{1}{(2\pi)^N}\int\cdots\int\left\{\hat{n}_N \times\left[\left\{\hat{n}_{N-1} \times \cdots \times\left[\left\{\hat{n}_2 \times\left[\left\{\hat{n}_1 \times \hat{a}\right\} \times \nabla \frac{e^{ik\left|\vec{r}_2-\vec{r}_1\right|}}{\left|\vec{r}_2-\vec{r}_1\right|}\right]\right\}\right]\right\}\right. \qquad (3.3\text{-}3)$$

$$\left. \times \nabla \frac{e^{ik\left|\vec{r}_3-\vec{r}_2\right|}}{\left|\vec{r}_3-\vec{r}_2\right|}\right]\right\}\times\cdots\Bigg\} \times \nabla \frac{e^{ik\left|\vec{r}_N-\vec{r}_{N-1}\right|}}{\left|\vec{r}_N-\vec{r}_{N-1}\right|}\Bigg]\Bigg\} \times \nabla \frac{e^{ik\left|\vec{R}-\vec{r}_N\right|}}{\left|\vec{R}-\vec{r}_N\right|}\, e^{ik\hat{k}\cdot\vec{r}_1}\, ds_1 \cdots ds_N.$$

Assume the wavelength to be so short that $k\left|\vec{r}_{j+1} - \vec{r}_j\right| >> 1$. For this case

$$\nabla \frac{e^{ik\left|\vec{r}_{j+1} - \vec{r}_j\right|}}{\left|\vec{r}_{j+1} - \vec{r}_j\right|} \approx - \frac{ike^{ik\left|\vec{r}_{j+1} - \vec{r}_j\right|}}{\left|\vec{r}_{j+1} - \vec{r}_j\right|^2} (\vec{r}_{j+1} - \vec{r}_j) . \tag{3.3-4}$$

In the integrand of (3.3-3) all of the quantities except the exponential factor can be replaced by their values at the specular reflection points. With this approximation, (3.3-3) becomes

$$\vec{H}_s = \left(\frac{k}{2\pi i}\right)^N \frac{\left\{\hat{n}_N \times \ldots \times \left[\left\{\hat{n}_2 \times \left[\left\{\hat{n}_1 \times \hat{a}\right\} \times \hat{R}_1\right]\right\} \times \hat{R}_2\right]\right\} \times \ldots \times \hat{R}_N}{R_1 R_2 \ldots R_N} \tag{3.3-5}$$

$$\times \int \ldots \int e^{ik\left[\hat{k} \cdot \vec{r}_1 + \sum_{j=1}^{N} R_j\right]} dS_1 \ldots dS_N$$

where

$$\vec{r}_{j+1} - \vec{r}_j = \vec{R}_j = R_j \hat{R}_j \text{ and } \vec{R} - \vec{r}_N = \vec{R}_N = R_N \hat{R}_N .$$

Let $\xi_1 = x_1, \xi_2 = y_1, \xi_3 = x_2, \xi_4 = y_2, \ldots, \xi_{2N-1} = x_N, \xi_{2N} = y_N,$

and expand the phase factor in Equation (3.3-5) in the ξ_j. The first order terms will vanish at the specular reflection points, leaving terms of second order as the leading terms in the expansion. Neglecting all but second order terms, (3.3-5) becomes

$$\vec{H}_s = \left(\frac{k}{2\pi i}\right)^N \frac{\cos\theta_1}{R_1} \frac{\cos\theta_2}{R_2} \ldots \frac{\cos\theta_N}{R_N} \hat{H}_N e^{ik\left[\hat{K} \cdot \vec{r} + \sum_{j=1}^{N} R_j\right]} I \tag{3.3-6}$$

where $I = \int_{-\infty}^{\infty} \cdots \int_{-\infty}^{\infty} e^{ik \underset{\sim}{\xi} \underset{\sim}{M} \underset{\sim}{\xi}} d\xi_1 \cdots d\xi_{2N}$

is a 2N-dimensional Fresnel integral, $\hat{H}_N$ is a unit vector giving the polarization of the scattered wave, and $\underset{\sim}{\xi}$ and M are the matrices

$$\underset{\sim}{\xi} = \begin{bmatrix} \xi_1 \\ \xi_2 \\ \vdots \\ \xi_{2N} \end{bmatrix} \quad \underset{\sim}{\xi}^{\sim} = \begin{bmatrix} \xi_1, & \xi_2, & \cdots, & \xi_{2N} \end{bmatrix} \tag{3.3-7}$$

$$\mathbf{M} = \tilde{\mathbf{M}} =$$

$$\begin{bmatrix}
\frac{\cos\theta_1}{\rho_{11}} + \frac{1-\sin^2\theta_1\cos^2\phi_1}{2R_1} & -\frac{\sin^2\theta_1\sin\phi_1\cos\phi_1}{2R_1} & \frac{\sin\theta_2\cos\phi_2\sin\theta_1\cos\phi_1-\alpha_{111}}{2R_1} & \cdots & 0 \\
-\frac{\sin^2\theta_1\sin\phi_1\cos\phi_1}{2R_1} & \frac{\cos\theta_1}{\rho_{12}} + \frac{1-\sin^2\theta_1\sin^2\phi_1}{2R_1} & \frac{\sin\theta_2\cos\phi_2\sin\theta_1\sin\phi_1-\alpha_{121}}{2R_1} & \cdots & 0 \\
\frac{\sin\theta_2\cos\phi_2\sin\theta_1\cos\phi_1-\alpha_{111}}{2R_1} & \frac{\sin\theta_2\cos\phi_2\sin\theta_1\sin\phi_1-\alpha_{121}}{2R_1} & \frac{\cos\theta_2}{2\rho_{21}}+(1-\sin^2\theta_2\cos^2\phi_2)\left(\frac{1}{2R_1}+\frac{1}{2R_2}\right) & \cdots & 0 \\
\frac{\sin\theta_2\sin\phi_2\sin\theta_1\cos\phi_1-\alpha_{112}}{2R_1} & \frac{\sin\theta_2\sin\phi_2\sin\theta_1\sin\phi_1-\alpha_{122}}{2R_1} & -\sin^2\theta_2\sin\phi_2\cos\phi_2\left(\frac{1}{2R_1}+\frac{1}{2R_2}\right) & \cdots & 0 \\
0 & 0 & \frac{\sin\theta_3\cos\phi_3\sin\theta_2\cos\phi_2-\alpha_{211}}{2R_2} & \cdots & 0 \\
0 & 0 & \frac{\sin\theta_3\sin\phi_3\sin\theta_2\cos\phi_2-\alpha_{212}}{2R_2} & \cdots & 0 \\
0 & 0 & 0 & \cdots & 0 \\
\vdots & \vdots & \vdots & \cdots & \vdots \\
0 & 0 & 0 & \cdots & -\frac{\sin^2\theta_N\sin\phi_N\cos\phi_N}{2R_{N-1}\left(\frac{R_N}{R_{N-1}+R_N}\right)} \\
0 & 0 & 0 & \cdots & \frac{\cos\theta_N}{\rho_{N2}}+\frac{1-\sin^2\theta_N\sin^2\phi_N}{2R_{N-1}\left(\frac{R_N}{R_{N-1}+R_N}\right)}
\end{bmatrix} \qquad (3.3\text{-}8)$$

In (3.3-8) α_{j11} is the cosine of the angle between the x_j and the x_{j+1} axes, α_{j12} is the cosine of the angle between the x_j and the y_{j+1} axes, α_{j21} is the cosine of the angle between the y_j and the x_{j+1} axes, and α_{j22} is the cosine of the angle between the y_j and y_{j+1} axes.

Evaluation of the integral I yields

$$I = \left(\frac{\pi e^{\frac{\pi i}{2}}}{k} \right)^N \frac{1}{\sqrt{|M|}} \tag{3.3-9}$$

where $|M|$ is the determinant of M. Thus (3.3-6) becomes

$$\vec{H}_s = \hat{H}_N \frac{e^{ik\left(\hat{k}\cdot\vec{r}_1 + \sum_{j=1}^{N} R_j\right)}}{\sqrt{|M|}} \tag{3.3-10}$$

When the radii of curvature at the reflection points are finite, Equation (3.3-10) is equivalent to Equation (3.1-1). To illustrate this equivalence, the method of Stationary Phase will be applied to the problem of multiple scattering from two spheres treated by Fock's method in section 3.2. In this problem

$$\begin{aligned} &\rho_{11} = \rho_{12} = \rho_{21} = \rho_{22} = r_0, \\ &R_1 = d - \sqrt{2}\, r_0, \\ &R_2 = z - \frac{r_0}{\sqrt{2}}, \\ &\Theta_1 = \Theta_2 = \frac{\pi}{4}, \\ &\hat{k}\cdot\vec{r}_1 = -\frac{r_0}{\sqrt{2}}, \end{aligned} \tag{3.3-11}$$

and

$$\begin{aligned} &\alpha_{111} = 1,\ \alpha_{112} = \alpha_{121} = \alpha_{122} = 0, \\ &\phi_1 = \frac{\pi}{2},\ \phi_2 = \frac{3\pi}{2}. \end{aligned}$$

Assuming that $d - \frac{r_o}{\sqrt{2}} << z$, the substitution of (3.3-11) into (3.3-8) gives

$$\left| M \right| = \frac{(2d - \sqrt{2}\, r_o)\, d}{8\, r_o^2\, (d - \sqrt{2}\, r_o)^2} \qquad (3.3\text{-}12)$$

The substitution of (3.3-11) and (3.3-12) into (3.3-10) gives

$$\vec{H}_s = \vec{H}_N \frac{r_o^2\, e^{ik(z + d - 2\sqrt{2}\, r_o)}}{4d(z - \frac{r_o}{\sqrt{2}})\sqrt{1 - \frac{r_o}{\sqrt{2}\, d}}} \; . \qquad (3.3\text{-}13)$$

If $\sqrt{2}\, z >> r_o$ Equation (3.3-13) reduces to Equation (3.2-26).

3.4 The Biconical Reflector.

In the examples considered thus far the radii of curvature of the scattering surfaces have either been all finite or all infinite. However, many problems that arise in practice involve both finite and infinite radii of curvature. Rather than attempt to give a general formula for all the cases that might arise, the scattering from a biconical reflector will be treated to illustrate the appropriate technique. A method of attack for this problem has already been given, namely the use of (2.1-4) with the value of $\vec{H}$ in the integrand given by the geometric optics formula (3.1-1). As with the examples which have already been treated, it is usually advantageous to make simplifying approximations in the evaluation of the integral appearing in (2.1-4). One approximation is to take into account only the current induced on the scattering surface by the last reflection of a multiply reflected ray. A second approximation is to use stationary phase in evaluating the integral whenever appropriate. In the following computation only the case of transmitter and receiver along the x-axis is considered (Figure 14).

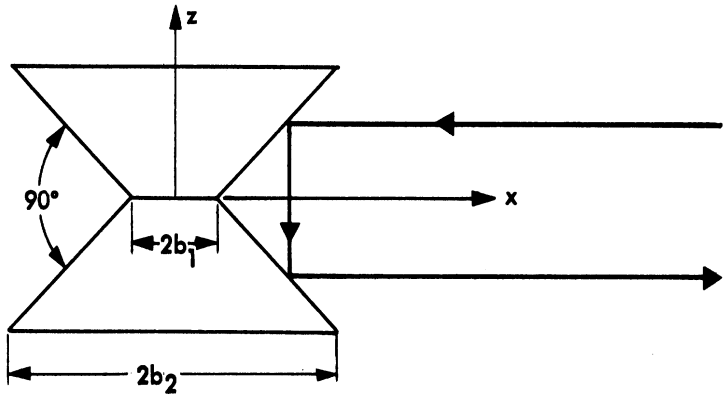

FIG. 14 THE BICONICAL REFLECTOR

The equation of the upper cone is

$$x^2 + y^2 = (z + b_1)^2 \tag{3.4-1}$$

while the equation of the lower cone is

$$x^2 + y^2 = (z - b_1)^2 . \tag{3.4-2}$$

Equation (3.1-1) can be used to obtain the field reflected from the upper cone to the lower cone. If the surface coordinates are z and ϕ, then

$$\begin{aligned} x &= (z + b_1)\cos\phi, \\ y &= (z + b_1)\sin\phi, \\ z &= z . \end{aligned} \tag{3.4-3}$$

The outward unit normal on the upper cone is

$$\hat{n} = \frac{\cos\phi}{\sqrt{2}}\hat{i}_x + \frac{\sin\phi}{\sqrt{2}}\hat{i}_y - \frac{1}{\sqrt{2}}\hat{i}_z . \tag{3.4-4}$$

Applying (3.1-7) yields

$$-\begin{bmatrix} G_{zz} & G_{z\phi} \\ G_{\phi z} & G_{\phi\phi} \end{bmatrix} = \begin{bmatrix} 0 & 0 \\ 0 & \frac{z + b_1}{\sqrt{2}} \end{bmatrix} . \tag{3.4-5}$$

The arc element is given by

$$d\sigma^2 = 2dz^2 + (z + b_1)\, d\phi^2 \tag{3.4-6}$$

so that

$$\begin{bmatrix} g_{zz} & g_{z\phi} \\ g_{\phi z} & g_{\phi\phi} \end{bmatrix} = \begin{bmatrix} 2 & 0 \\ 0 & (z + b_1)^2 \end{bmatrix} . \tag{3.4-7}$$

The inverse of the metric tensor is

$$\begin{bmatrix} g^{zz} & g^{z\phi} \\ g^{\phi z} & g^{\phi\phi} \end{bmatrix} = \begin{bmatrix} 1/2 & 0 \\ 0 & \frac{1}{(z + b_1)^2} \end{bmatrix} . \tag{3.4-8}$$

The phase factor is

$$\Omega(z, \phi) = -x = -(z + b_1)\cos\phi . \tag{3.4-9}$$

The derivatives of the phase factor are

$$\Omega_z = -\cos\phi, \qquad \Omega_\phi = (z + b_1)\sin\phi . \tag{3.4-10}$$

The Christoffel symbols of the first kind are

$$[z, z; z] = [z, z; \phi] = [z, \phi; z] = [\phi, \phi; \phi] = 0 , \tag{3.4-11}$$
$$[\phi, \phi; z] = -(z + b_1) = -[\phi, z; \phi].$$

The Christoffel symbols of the second kind are

$$\Gamma^z_{zz} = \Gamma^\phi_{zz} = \Gamma^z_{z\phi} = \Gamma^\phi_{\phi\phi} = 0,$$
$$\Gamma^z_{\phi\phi} = -(1/2)(z + b_1) , \tag{3.4-12}$$
$$\Gamma^\phi_{\phi z} = \frac{1}{z + b_1}$$

so that

$$\begin{bmatrix} \Omega_{zz} & \Omega_{z\phi} \\ \Omega_{\phi z} & \Omega_{\phi\phi} \end{bmatrix} = \begin{bmatrix} 0 & 0 \\ 0 & (1/2)(z + b_1)\cos\phi \end{bmatrix} . \tag{3.4-13}$$

Since $\cos\zeta = \hat{i}_x \cdot \hat{n} = \cos\phi/\sqrt{2}$,

$$\begin{bmatrix} T_{zz} & T_{z\phi} \\ T_{\phi z} & T_{\phi\phi} \end{bmatrix} = \begin{bmatrix} 2 - \cos^2\phi & (z + b_1)\sin\phi\cos\phi \\ (z + b_1)\sin\phi\cos\phi, & (z + b_1)^2\cos^2\phi + R_1(z + b_1)\cos\phi \end{bmatrix} , \tag{3.4-14}$$

$$\begin{bmatrix} T^z_z & T^z_\phi \\ T^\phi_z & T^\phi_\phi \end{bmatrix} = \begin{bmatrix} 1 - (1/2)\cos^2\phi & (1/2)(z + b_1)\sin\phi\cos\phi \\ \dfrac{\sin\phi\cos\phi}{z + b_1} & \cos^2\phi + \dfrac{R_1\cos\phi}{z + b_1} \end{bmatrix}$$

where R_1 is the distance from the specular reflection point on the upper cone.

Thus

$$D(R_1) = (1/2)\cos^2\phi \left[1 + \frac{R_1}{z + b_1}\left(\frac{2}{\cos\phi} - \cos\phi\right)\right]. \tag{3.4-15}$$

If the magnetic field incident on the upper cone is $\hat{i}_y e^{-ikx}$, then the magnetic field scattered from the upper cone is

$$\frac{(-\sin\phi\cos\phi\hat{i}_x + \cos^2\phi\hat{i}_y + \sin\phi\hat{i}_z)\, e^{ik\left[R_1 - (z + b_1)\cos\phi\right]}}{\sqrt{1 + \frac{R_1}{z + b_1}\left(\frac{2}{\cos\phi} - \cos\phi\right)}}. \tag{3.4-16}$$

For $\phi = \Theta$ the reflected magnetic field on the surface of the lower cone is

$$\sqrt{\frac{z + b_1}{3z + b_1}}\, e^{ik(z - b_1)}\hat{i}_y \tag{3.4-17}$$

where z is the height at which the incident ray strikes the upper cone. If (3.4-16) is written in terms of the coordinates x', y', z' on the lower cone with

$$\begin{aligned} x' &= (b_1 - z')\cos\phi', \\ y' &= (b_1 - z')\sin\phi' \end{aligned} \tag{3.4-18}$$

it becomes

$$\sqrt{\frac{b_1 - z'}{b_1 - 3z'}}\, e^{ik\left[-b_1 - z' + (1/2)\left\{\frac{(b_1 - z')^2}{b_1 - 3z'}\right\}\phi'^2 + O(\phi'^4)\right]}\left[\hat{i}_y + O(\phi')\right] \tag{3.4-19}$$

where $O(X)$ is a function for which $\lim_{x \to 0} O(x)/x$ = constant which is neither zero nor infinity. If (3.4-19) is used in (2.1-2) and the integration over ϕ' is carried out by the method of stationary phase, it is found that the doubly scattered field at a large distance x is given by

$$\hat{i}_y \frac{ik}{2\pi} \frac{e^{ik(x - 2b_1)}}{x} \int_0^{b_2 - b_1} \frac{(b_1 + z)^{3/2}}{(b_1 + 3z)^{1/2}} \int_{-\infty}^{\infty} e^{ik \frac{(b_1 + z)(b_1 + 2z)}{b_1 + 3z} \phi'^2} d\phi' \, dz$$

(3.4-20)

$$= \sqrt{\frac{k}{\pi}} \frac{1}{2} e^{\frac{3\pi i}{4}} \hat{i}_y \frac{e^{ik(x - 2b_1)}}{x} \int_0^{b_2 - b_1} \frac{b_1 + z}{\sqrt{b_1 + 2z}} dz .$$

Integrating the last expression with respect to z gives

$$\frac{1}{3} \sqrt{\frac{2}{\lambda}} e^{\frac{3\pi i}{4}} \frac{e^{ik(x - 2b_1)}}{x} \left(b_2 \sqrt{2b_2 - b_1} - b_1^{3/2}\right) \hat{i}_y . \qquad (3.4\text{-}21)$$

Therefore, taking into account the radiation reflected from the lower cone to the upper cone, the radar cross-section of the biconical reflector is

$$\sigma = \frac{32\pi}{9\lambda} \left(b_2 \sqrt{2b_2 - b_1} - b_1^{3/2}\right)^2 . \qquad (3.4\text{-}22)$$

Numerically, the cross-section given by Equation (3.4-22) is in excellent agreement with experimental results that appear in Reference 5. Furthermore, the dependence on wave length is in agreement with Robertson's experimental results.

IV

EXPERIMENTAL DATA ON MULTIPLE SCATTERERS

Many experimental measurements have been made of the radar cross-section of the corner reflector. Of the bodies considered in this paper, data are available for square and triangular corner reflectors (Ref. 8) and for biconical reflectors (Ref. 5). In addition, the effects of compensation (Sec. 2.5) are discussed in detail in Reference 5. The material in this section is taken from these two references.

Theoretical curves and experimental points for the back-scattering from square and triangular corner reflectors are shown in Figures 15 and 16 respectively. The results are plotted so as to be independent of the size of the corner. The experimental dependence of the cross-section on the size of the reflector is shown in Table 1 for a square corner reflector.

TABLE 1

Variation of Cross-Section with Corner Side Length b
(λ = 9.1 cm)

Size of Reflector	Value of n in $\sigma = Kb^n$
6 inch	3.3
2 foot	4.0
3 foot	3.8
4 foot	3.8

A one foot corner reflector was used to obtain the constant K. For the 6 inch reflector, whose dimensions are of the same order of magnitude as the wavelength of the incident radiation, the cross-section deviated from that predicted by physical optics by a factor of approximately 1.6. The discrepancies between physical optics theory and experiment for the 3 and 4 foot reflectors can be attributed to non-perpendicularity of the reflector sides.

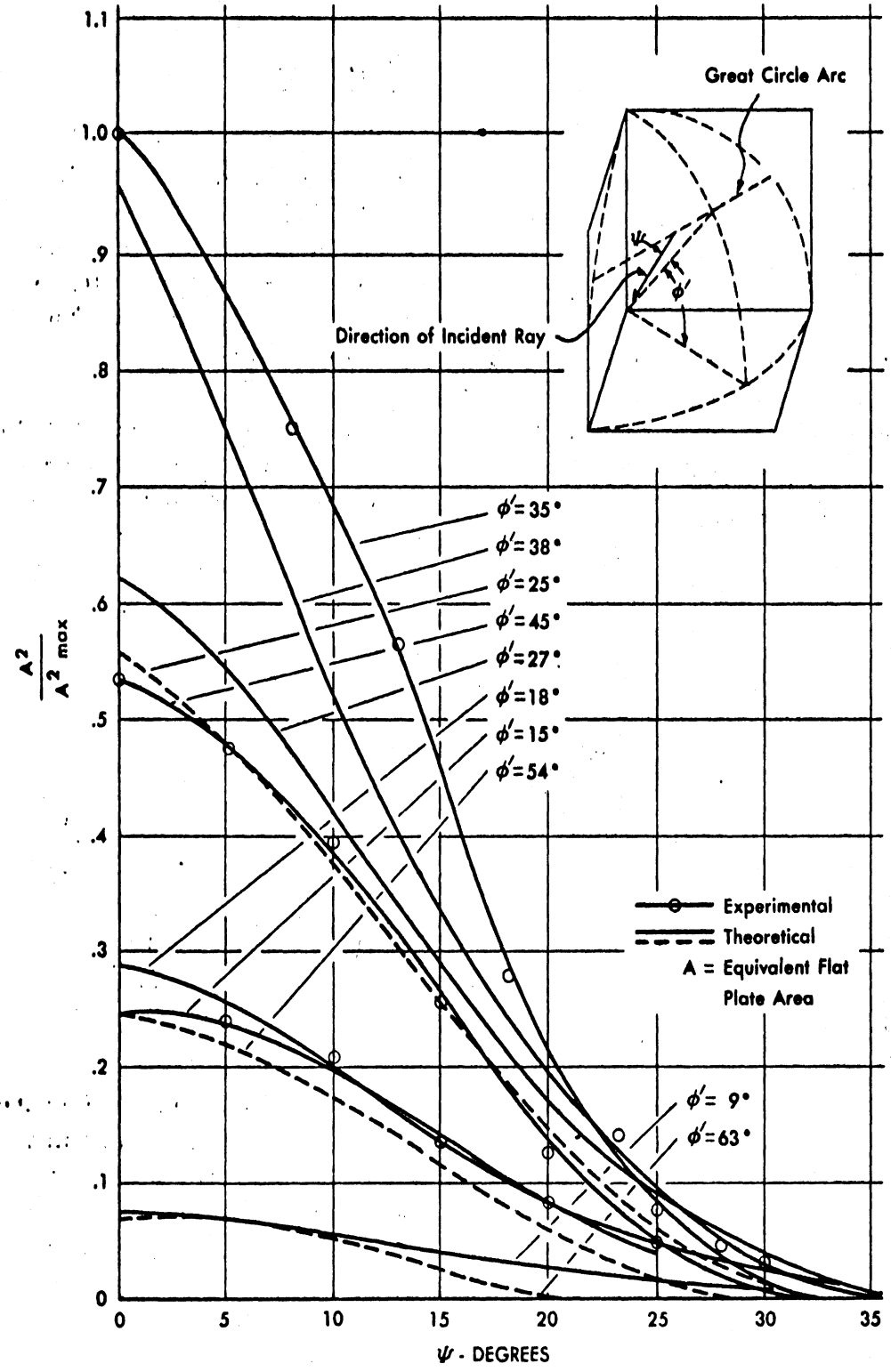

FIG. 15 RELATIVE INTENSITY OF REFLECTION FROM SQUARE CORNER REFLECTOR

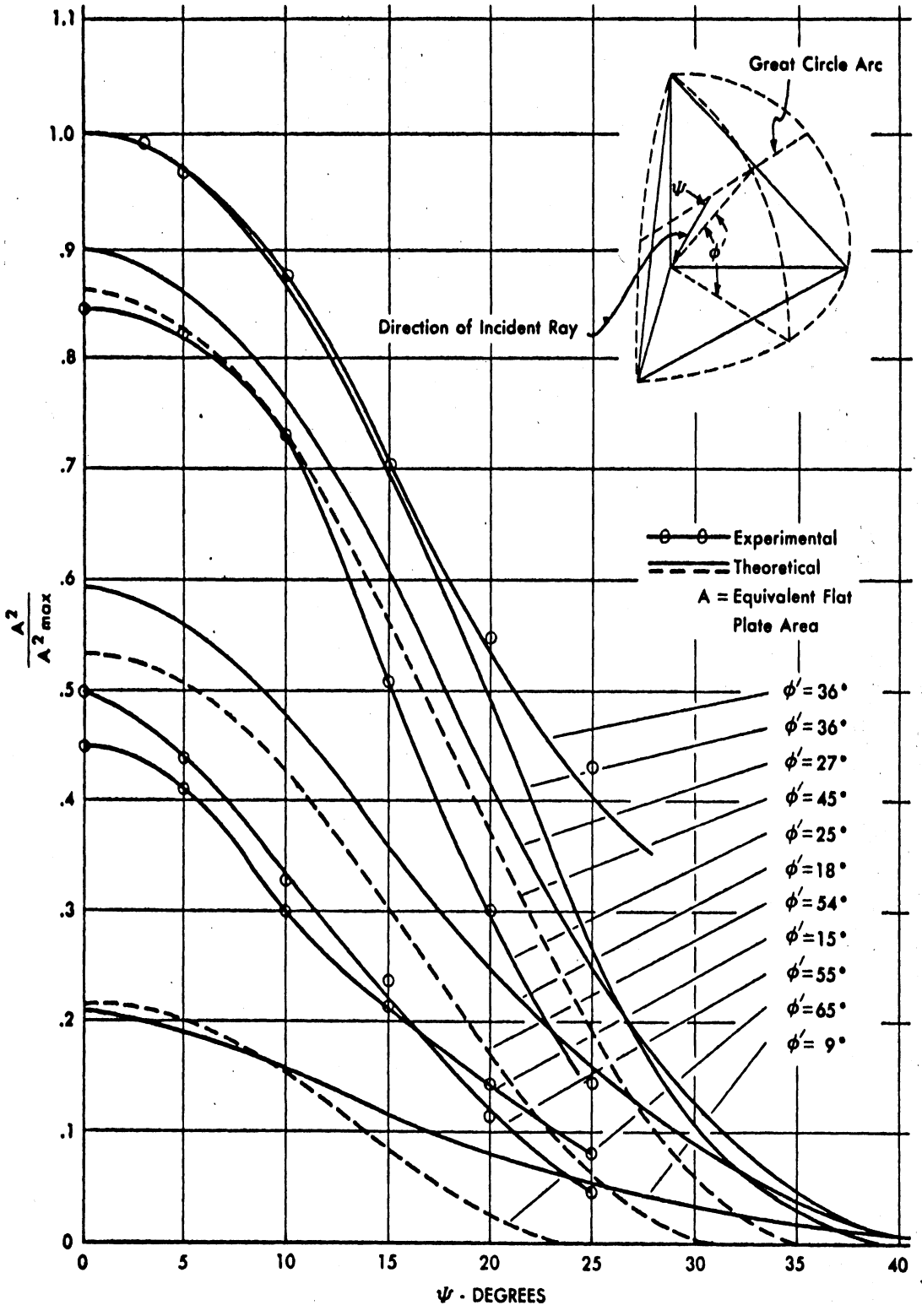

FIG. 16 RELATIVE INTENSITY OF REFLECTION FROM TRIANGULAR CORNER REFLECTOR

Compensation, i.e., reduction of scattering surface, can be used to widen the response pattern of a corner reflector (Sec. 2.5). The response pattern of the compensated triangular reflector, shown in Figure 17, is compared with the response pattern from an uncompensated reflector of the same dimensions in Figure 18. A special case of the compensated corner reflector is the corner which has been modified so as to yield a minimum response along the axis of symmetry (which usually yields the maximum response). The response pattern from this corner (Fig. 19) is shown in Figure 20.

The response pattern from a biconical reflector is shown in Figure 21. This response pattern is independent of azimuth since the biconical reflector is axially symmetric.

In conclusion it is felt that the profusion of multiple scatterers and the widespread use of corner reflectors warrants theoretical investigations, even though the corner reflector may be a poorer standard than the sphere since its exact solution is not known. This paper shows that when $\lambda < h$ the cross-section of these bodies can be predicted within an order of magnitude.

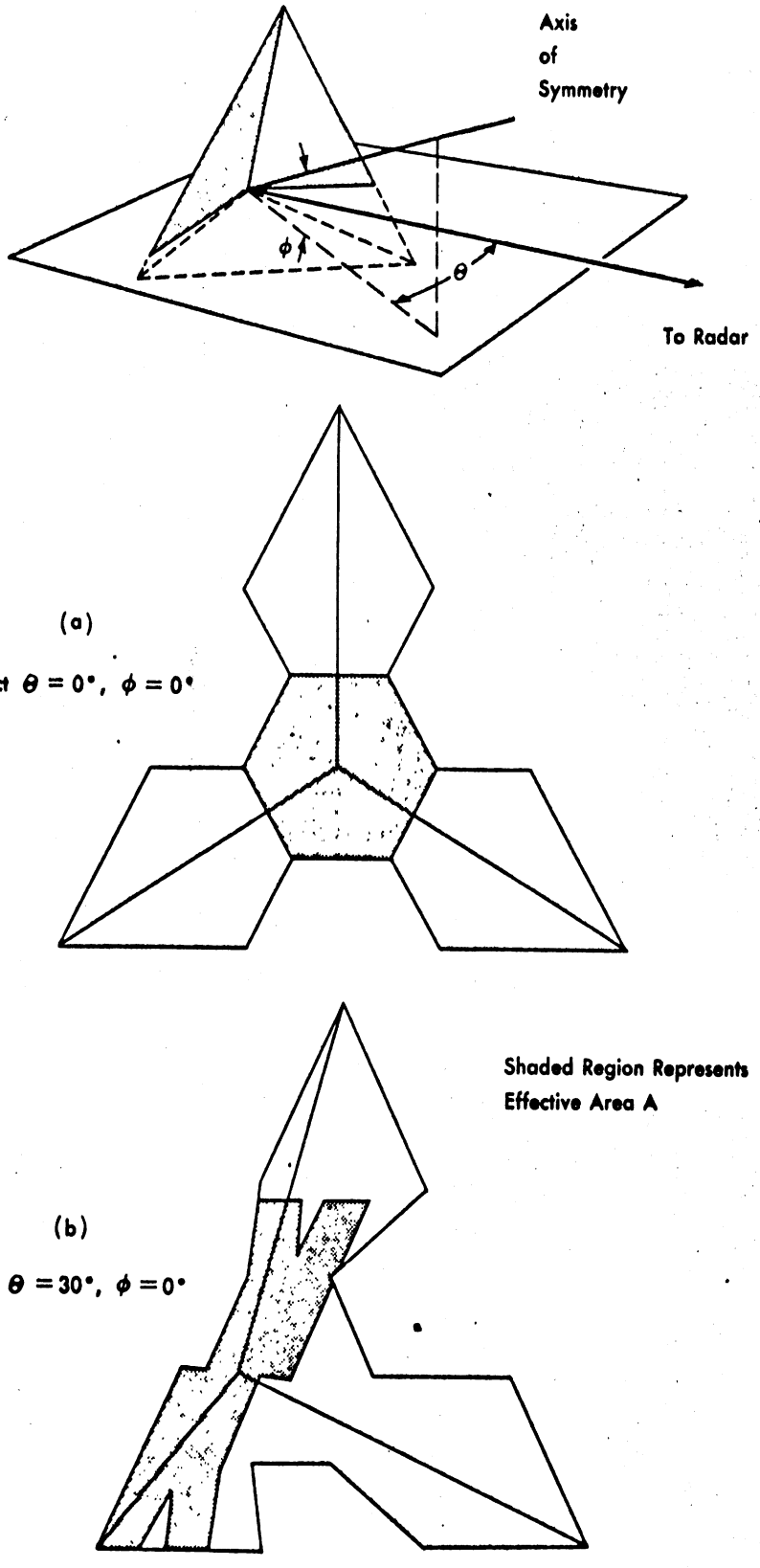

FIG. 17 COMPENSATED TRIANGULAR CORNER REFLECTOR

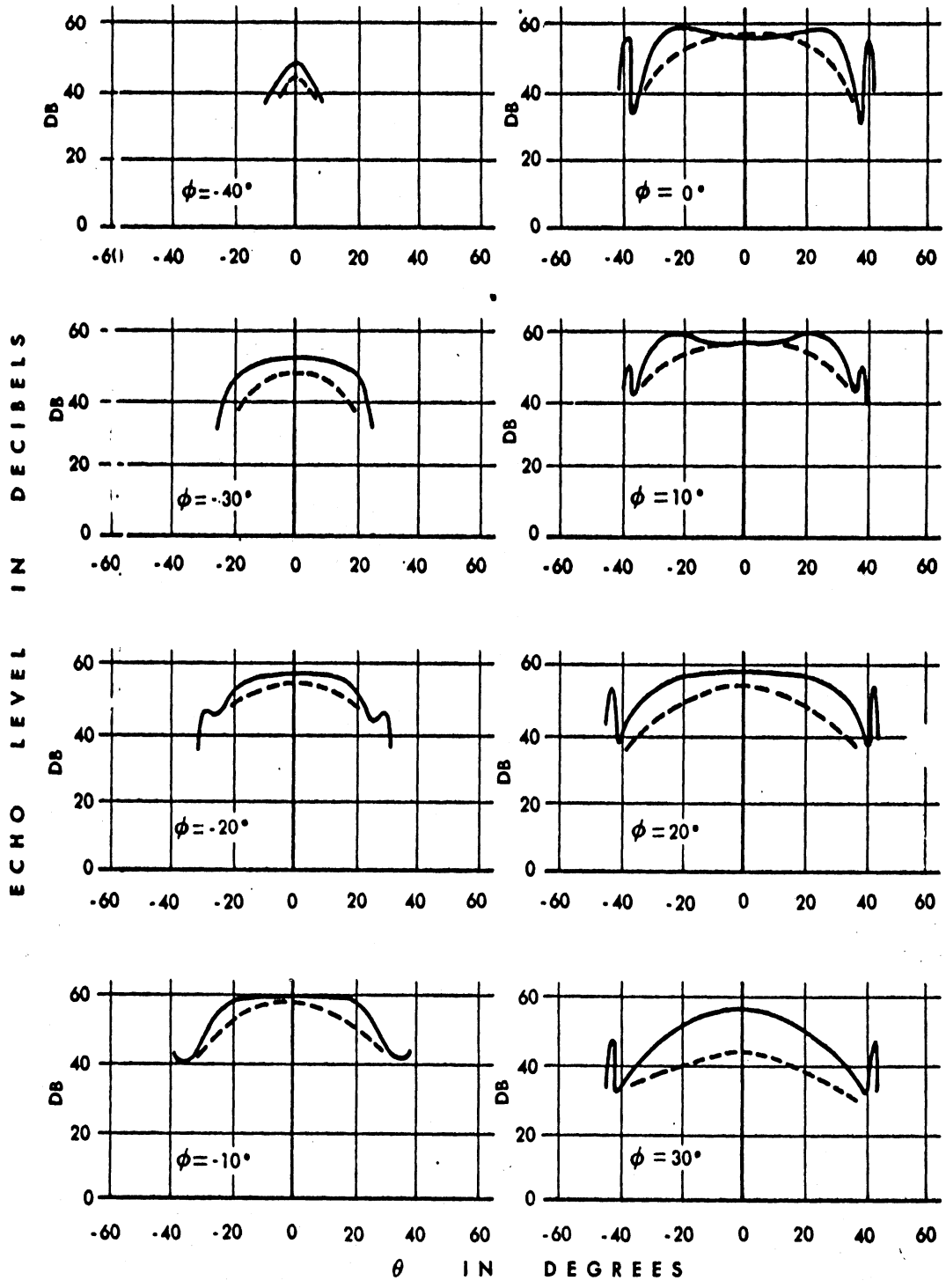

Compensated Reflector ——————
Uncompensated Reflector - - - - - -

FIG. 18 REFLECTION CHARACTERISTICS OF COMPENSATED TRIANGULAR CORNER REFLECTOR

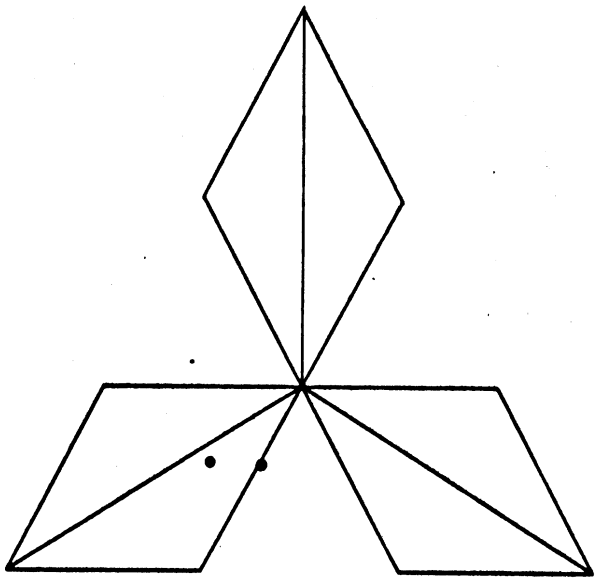

Aspect $\theta = 0°$, $\phi = 0°$
Effective Area, $A = 0$

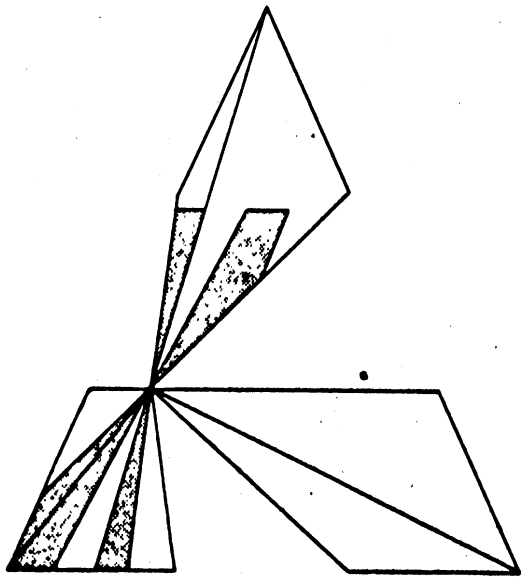

Aspect $\theta = 30°$, $\phi = 0°$
Shaded Region Represents Effective Area A

FIG. 19 SPECIALLY COMPENSATED TRIANGULAR CORNER REFLECTOR DESIGNED TO PRODUCE MINIMUM BACK-SCATTERING ALONG AXIS OF SYMMETRY

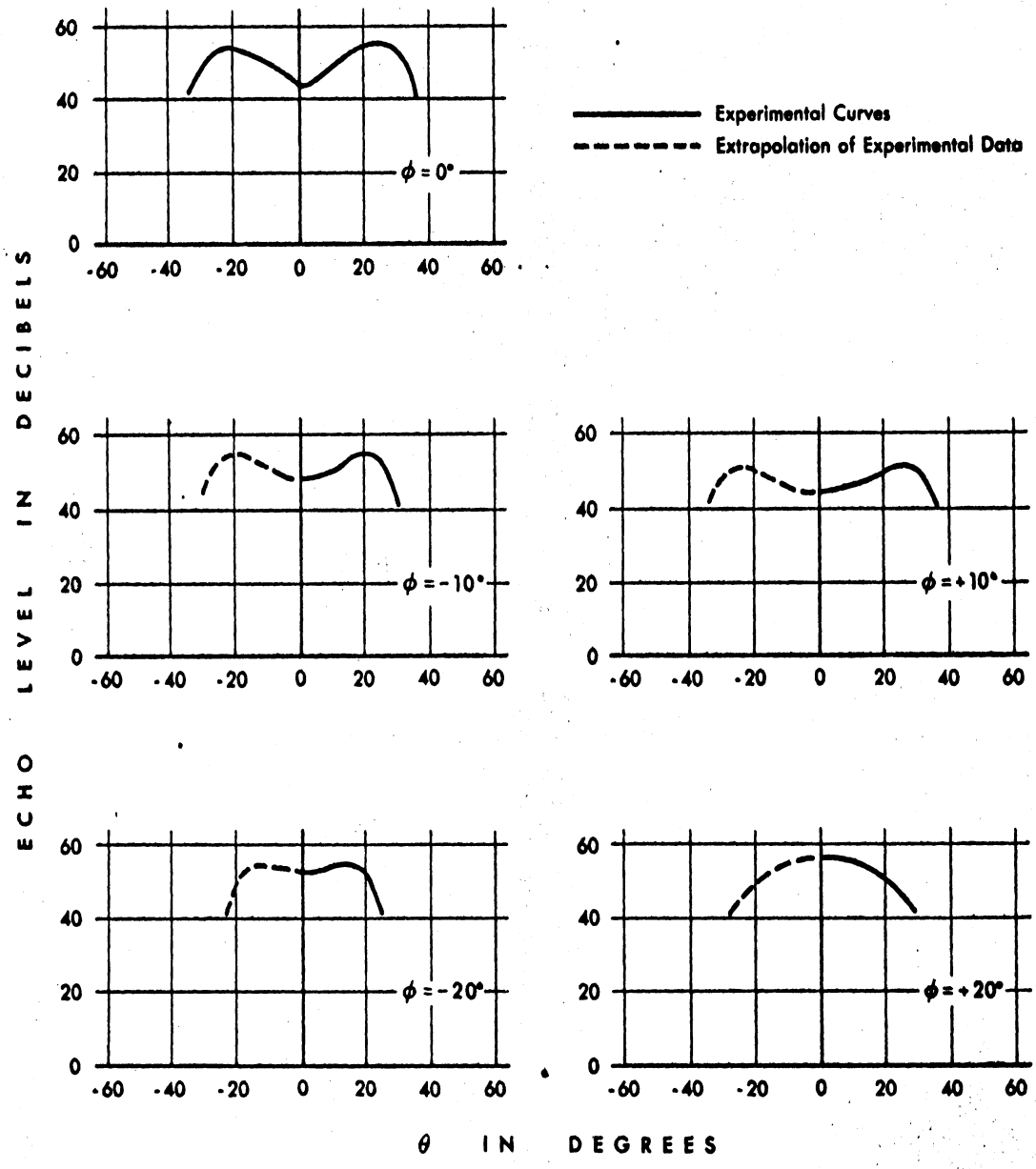

FIG. 20 RESPONSE PATTERN OF CORNER REFLECTOR DESIGNED FOR MINIMUM ECHO ON THE AXIS

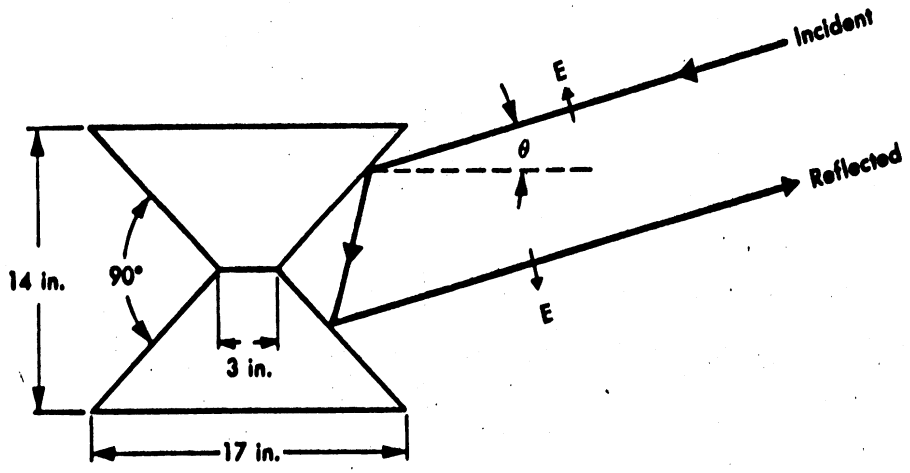

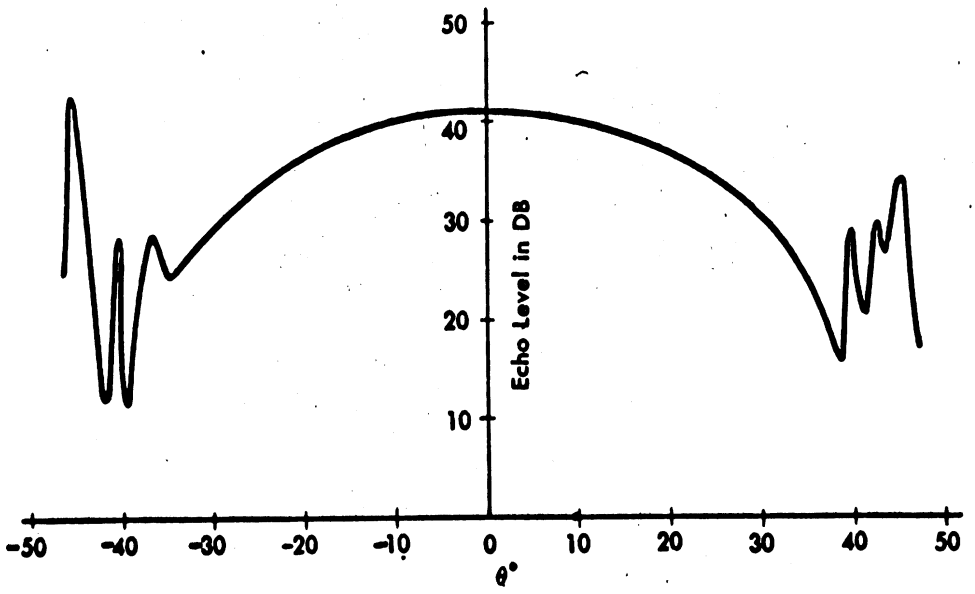

FIG. 21 RESPONSE PATTERN OF BICONICAL REFLECTOR

REFERENCES

1. "Mathematical Theory of Optics" by R. K. Luneberg, Brown University, Providence, R.I. (1944).

2. "A Note on the Foundations of Geometrical Optics" by N. Arley, Det Kgl. Danske Videnskabernes Selskab. Matematisk - fysiske Meddelser, Vol. 22, No. 8. (1945-46).

3. Electromagnetic Theory by J. A. Stratton, McGraw-Hill, New York, (1941).

4. ATI-5763, "Optical Theory of the Corner Reflector", by R. C. Spencer, MIT Radiation Laboratory. (1944).

5. "Targets for Microwave Radar Navigation" by S. D. Robertson, Bell System Technical Journal, 26, 852. (1947).

6. "Symposium on Microwave Optics", Eaton Electronics Research Laboratory, McGill University. (June 1953).

7. "Generalization of the Reflection Formulae to the Case of Reflection of an Arbitrary Wave from a Surface of Arbitrary Form", by V. A. Fock, Zhurnal Eksperimental' noi i Teoreticheskoi Fiziki, 20, 961, (1950).

8. RL-280, "The Application of Corner Reflectors to Radar (Experimental)" by R. D. O'Neal, M.I.T. Radiation Laboratory (1 July 1943).

APPENDIX

THE USE OF CORNER REFLECTORS FOR CAMOUFLAGE

The corner reflector, because of its large back-scattering cross-section, has long been used as a device for creating false radar echoes. This technique has been employed primarily by bomber aircraft for confusing search radars and tracking radars used in air defense. Dr. R. D. O'Neal, Assistant Division Manager of the Fort Worth Division of Consolidated Vultee Aircraft Corp., and others** have suggested the use of corner reflectors for camouflaging geographic features (such as bodies of water, cities, terrain irregularities, and large military or industrial installations) against recognition by means of navigation and bomb-sight radars.

To test the feasibility of such camouflage, an experiment was carried out recently by Consolidated Vultee in which an attempt was made to divide Eagle Mountain Lake, near Fort Worth, Texas, in half when seen by an AN/APS-23 X-band navigation and bombing radar. This experiment, which is described in Figures A-1 through A-7 inclusive,* met with striking success. The results of this test show clearly that the use of corner reflectors for camouflage merits further investigation.

---

*These figures are presented here through the courtesy of Dr. O'Neal and the Consolidated Vultee Aircraft Corporation.

**Dr. O'Neal points out that Mr. L. H. Moffatt of Consolidated Vultee Aircraft Corp. originated the idea independently at Consolidated Vultee Aircraft Corp. and had much to do with getting the program started there.

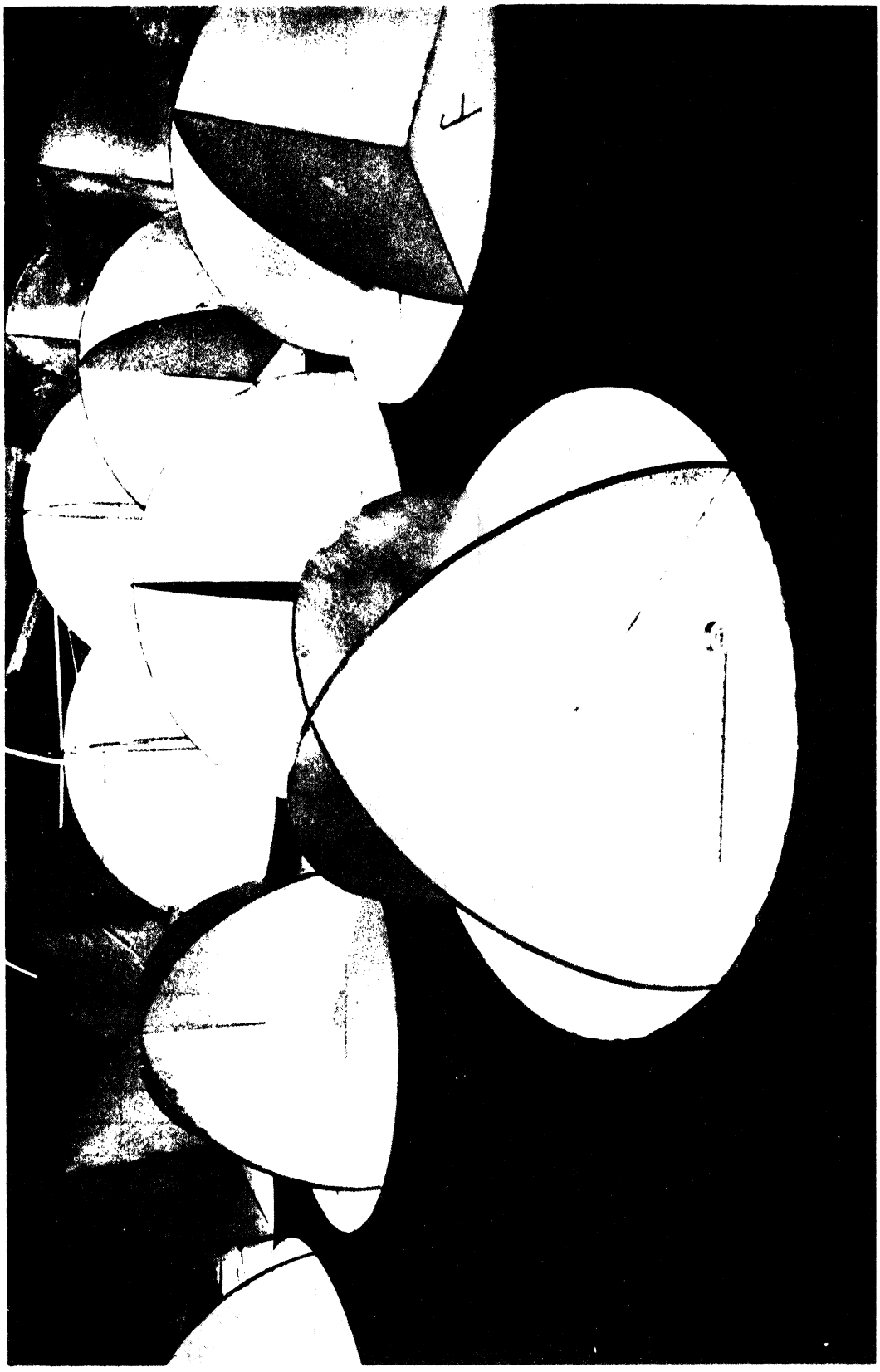

FIG. A-1 45-INCH DIAMETER CORNER REFLECTORS USED IN CAMOUFLAGE EXPERIMENTS

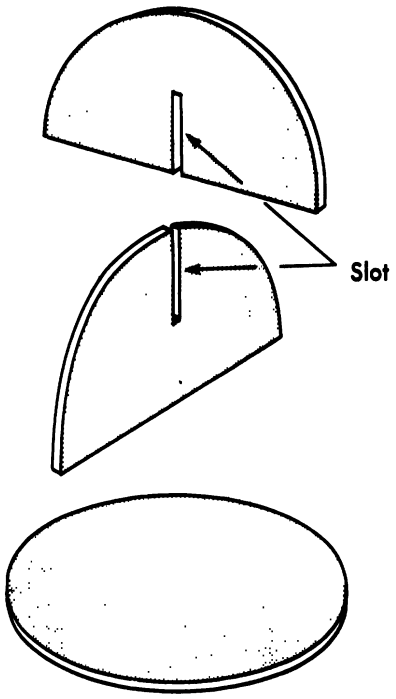

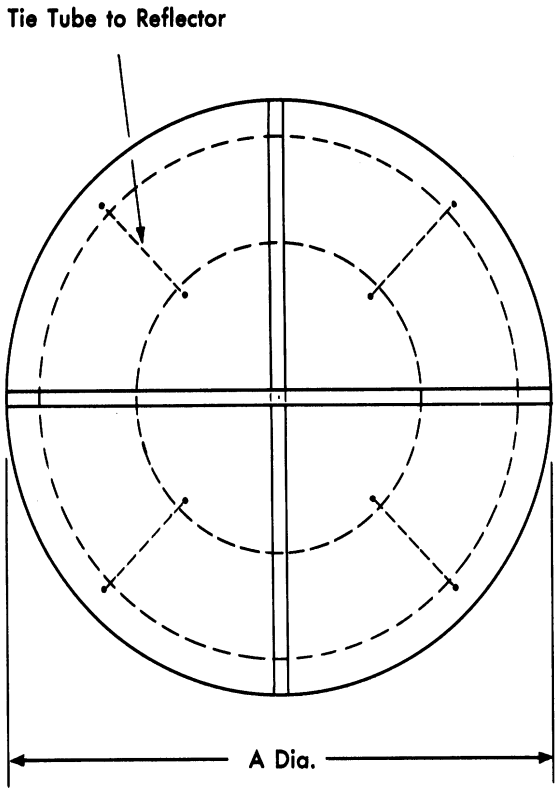

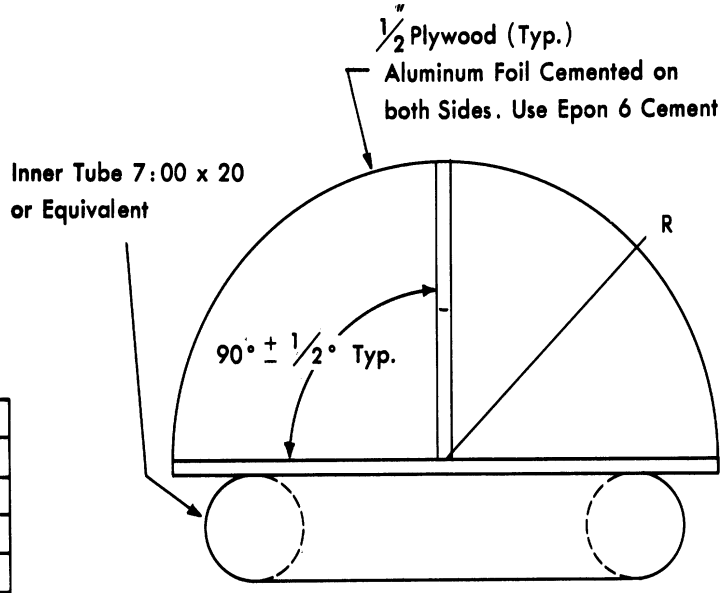

Dash No		A
-6		30 "
-8		20 "
-10		45 "

1 Screw and Glue Plywood Discs

2 Spray Aluminum Foil after Completion with Light Coat of Zinc Chromate Primer

FIG. A-2 SCHEMATIC DRAWING OF CORNER REFLECTOR ASSEMBLY

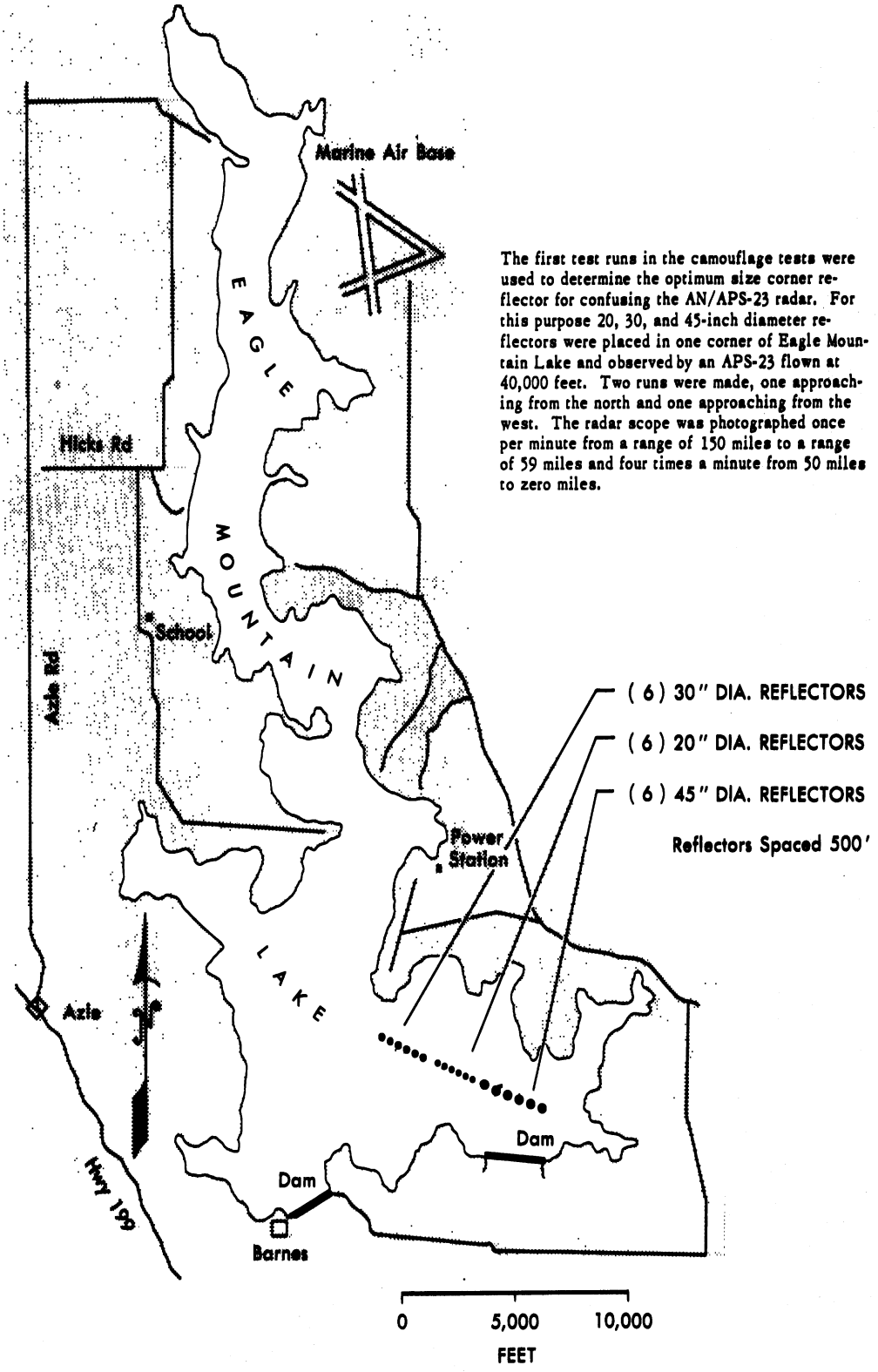

FIG. A-3 GEOGRAPHY OF EAGLE MOUNTAIN LAKE SHOWING FIRST TEST ARRANGEMENT

FIG. A-4 TYPICAL PPI PHOTO, FIRST TEST ARRANGEMENT

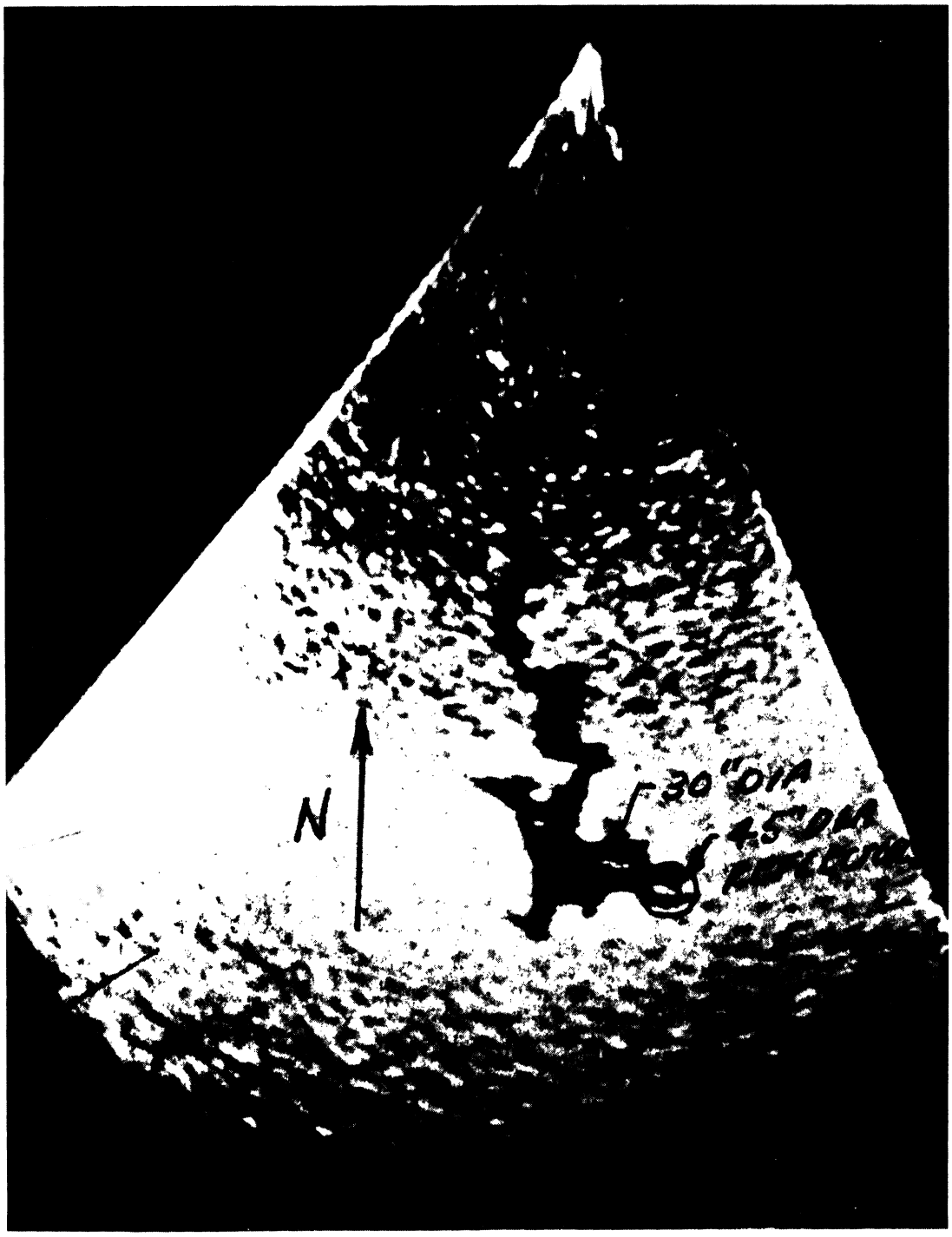

FIG. A-5a SECTOR PPI PHOTO, FIRST TEST ARRANGEMENT
30-MILE RANGE NORTH-SOUTH RUN

It can be seen from these photographs (Figs. A-5a and A-5b) that the 45-inch diameter reflectors are more effective than the 30-inch diameter reflectors and that the return obtained is independent of the direction of flight.

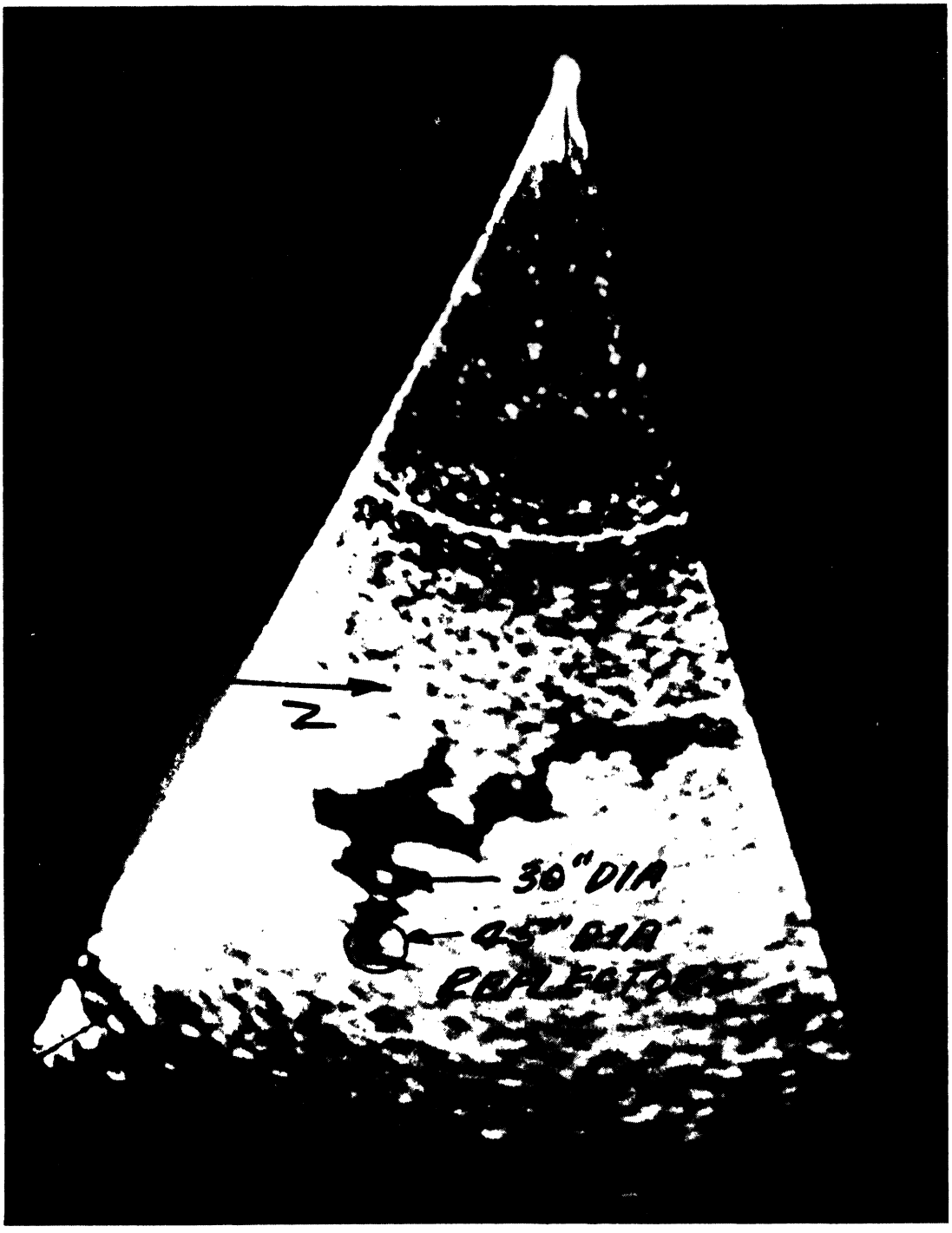

FIG. A-5b SECTOR PPI PHOTO, FIRST TEST ARRANGEMENT
25-MILE RANGE WEST-EAST RUN

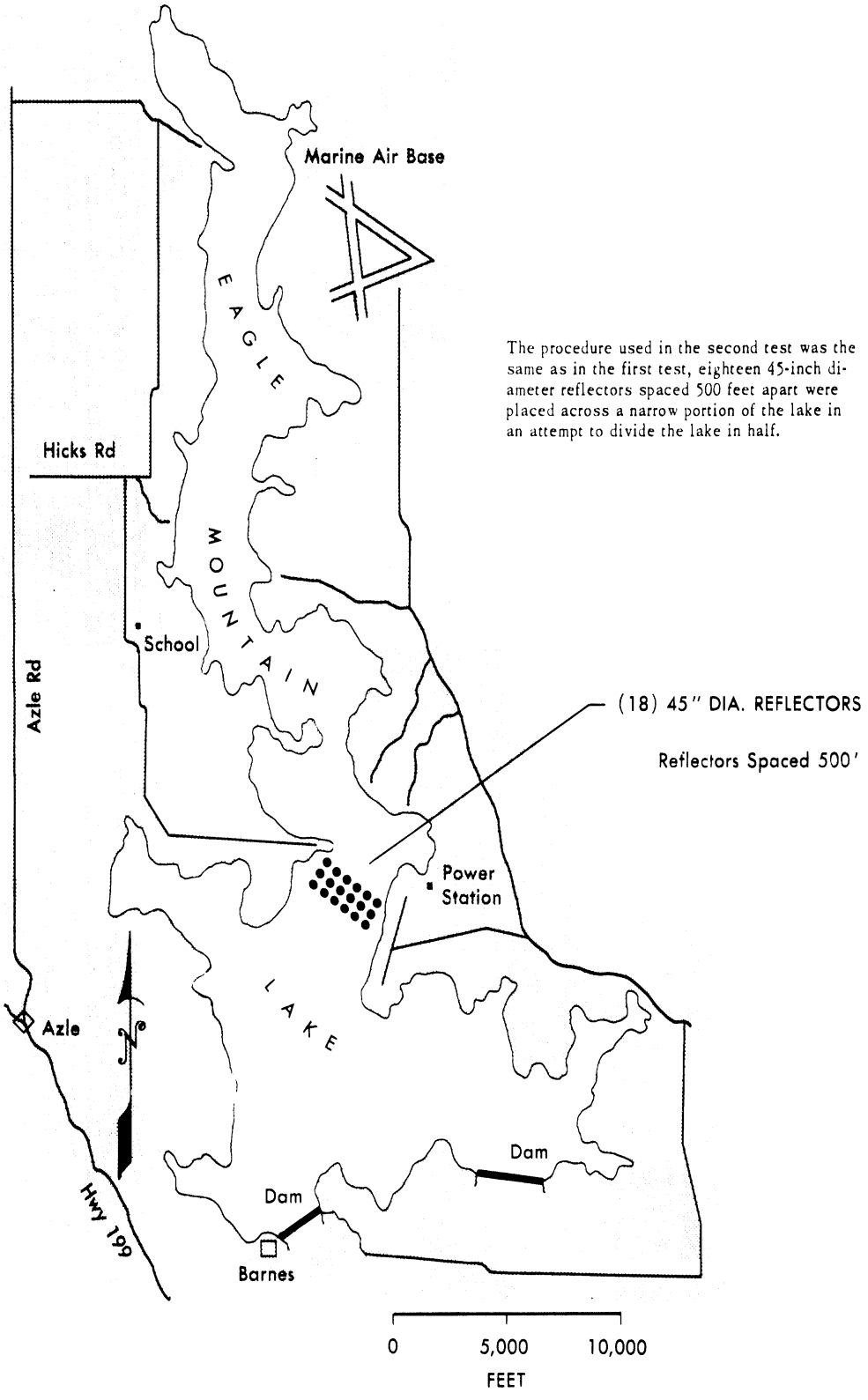

The procedure used in the second test was the same as in the first test, eighteen 45-inch diameter reflectors spaced 500 feet apart were placed across a narrow portion of the lake in an attempt to divide the lake in half.

FIG. A-6 SECOND TEST ARRANGEMENT

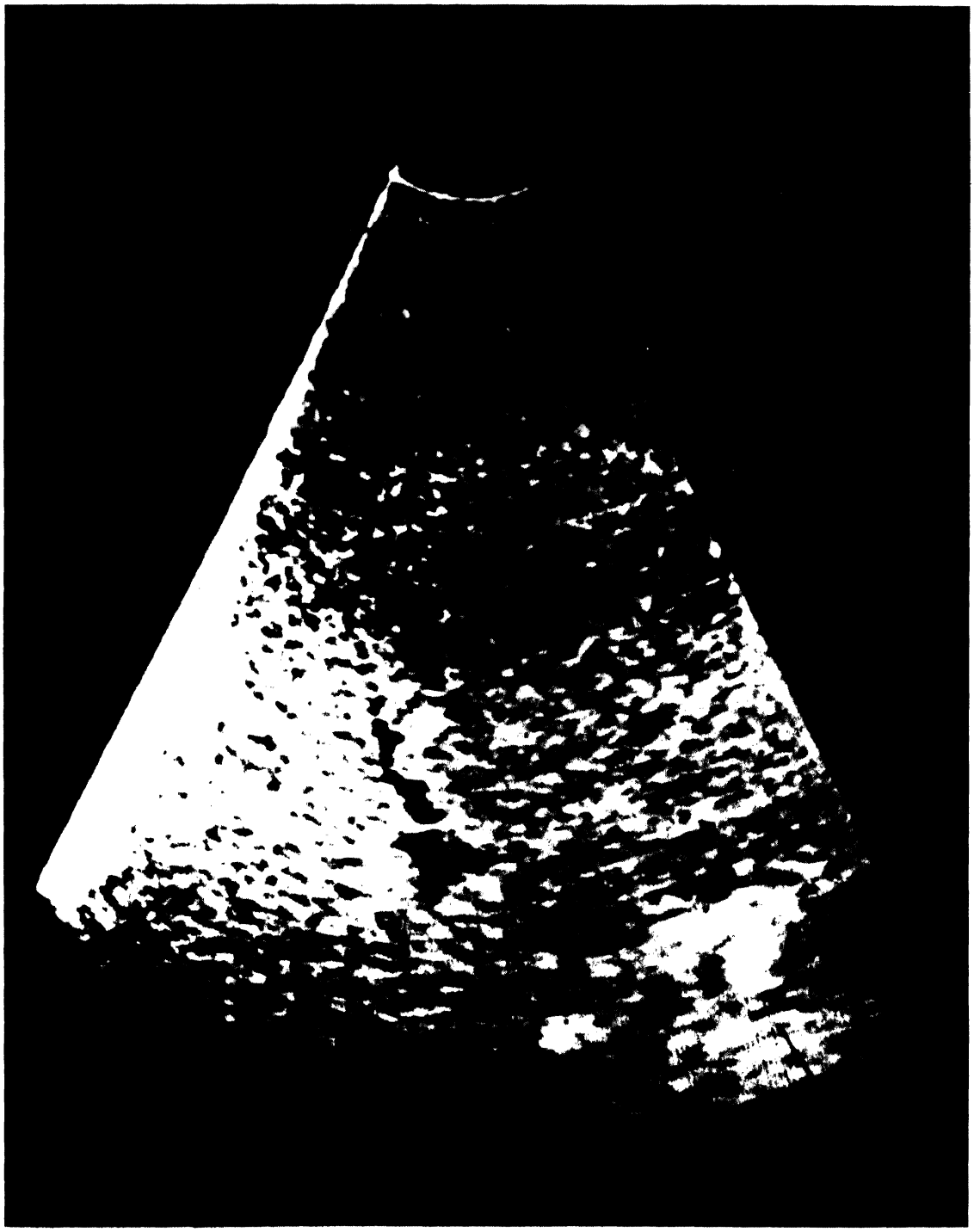

FIG. A-7a SECTOR PPI PHOTO, SECOND TEST ARRANGEMENT
30-MILE RANGE NORTH-SOUTH RUN

Both these photographs (Figs. A-7a and A-7b) show the rearrangement obtained by use of the corner reflectors. In both cases, Eagle Mountain Lake is seen as two separate lakes.

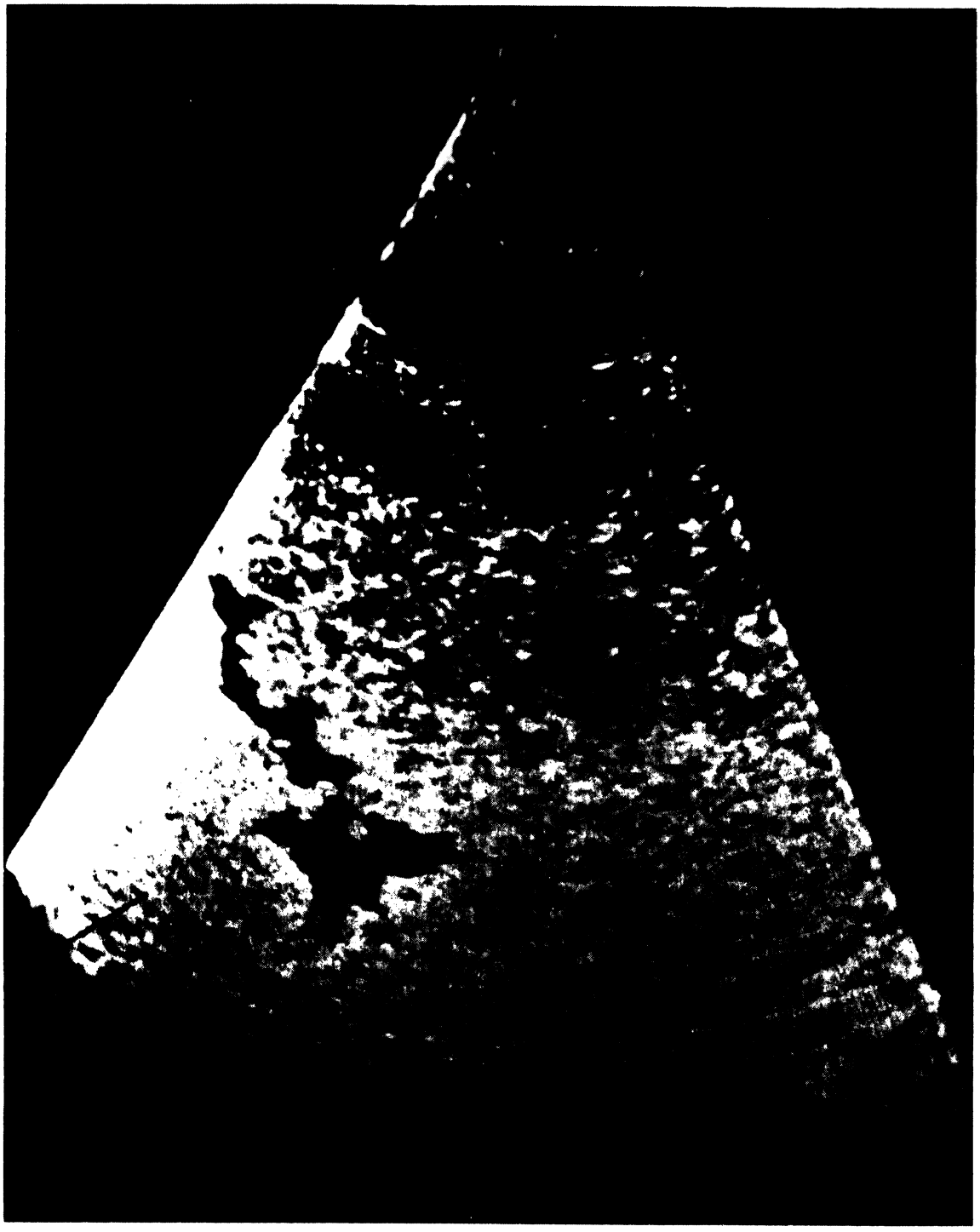

FIG. A-7b SECTOR PPI PHOTO, SECOND TEST ARRANGEMENT
17-MILE RANGE NORTH-SOUTH RUN